University of Zurich[UZH]

Department of Geography

Scaling from Plant Phenology to Land Surface Phenology at Biodiversity Test Sites, Using Phenocam and Satellite Imagery

GEO 511 Master's Thesis

Tobias Klee
11-718-350

Supervised by
Dr. Rogier de Jong

Faculty representative
Prof. Dr. Michael E. Schaepman

20. April 2018
Department of Geography, University of Zurich

Abstract

Vegetation phenology is an important indicator for climate change and biodiversity. Linking plant phenology (PP) and land surface phenology (LSP) has been a challenge due to their different spatial and temporal scales. The emergence of phenocams and high spatial-resolution satellite imagery like provided by Sentinel 2 opened up new perspectives to combine observations at species level with a large-scale coverage.

In this thesis, near surface and satellite remote sensing based measurements of phenology at biodiversity test sites have been compared, in an effort to observe PP and biodiversity with phenocam and Sentinel-2 imagery and to compare it to LSP data, using Landsat 8 and Moderate-Resolution Imaging Spectroradiometer (MODIS).

The analysis revealed that biodiversity in terms of functional groups of plant species can be detected with the proposed methods. Green-up patterns for the mixed deciduous forest at the Laegern test site showed a variation range of more than two weeks and for the tundra in Kytalyk up to one week, both in the phenocam and in the Sentinel-2 data. However, due to the different measurement techniques, the phenology transition dates differed considerably.

Comparing small-scale PP with larger-scale LSP measurements showed an overall correspondence between the metrics from the different datasets within about two weeks. Furthermore, qualitative characteristics like the field of view (FOV), the camera angle and atmospheric influences as well as methodical influences of the data preparation and processing have been evaluated.

A comparison between the two employed indices green chromatic coordinates (GCC) and normalised difference vegetation index (NDVI) has shown that NDVI detects an earlier increase of vegetation activity than GCC during the green-up period and a longer activity during senescence, mainly because NDVI is more sensitive for photosynthesis than greenness. This illustrates the definition issues that attend phenological studies: photosynthetic activity and greenness may reflect different ecological processes.

Contents

List of Figures

List of Tables

List of Abbreviations

API	Application Programming Interface
AVHRR	Advanced Very High Resolution Radiometer
CC	Chromatic Coordinates
DN	Digital Number
DOY	Day of Year
EOS	End of Growing Season
ESA	European Space Agency
ExGr	Excess Green Index
FOV	Field of View
GCB	Global Change and Biodiversity
GCC	Green Chromatic Coordinates
GEE	Google Earth Engine
GSL	Growing Season Length
L8	Landsat 8
LOS	Length of Growing Season
LSP	Land Surface Phenology

MODIS	Moderate-Resolution Imaging Spectroradiometer
NASA	National Aeronautics and Space Administration
NDVI	Normalised Difference Vegetation Index
NOAA	National Oceanic and Atmospheric Administration
PP	Plant Phenology
RCC	Red Chromatic Coordinates
RGB	Red-Green-Blue
RMSE	Root Mean Square Error
ROI	Region of Interest
S2	Sentinel 2
S2L8	Merged Sentinel-2 and Landsat-8 Dataset
SOS	Start of Growing Season
SR	Surface Reflectance
TOA	Top of Atmosphere
URPP	University Research Priority Program
UZH	University of Zurich

1 Introduction

1.1 Definition

Plant phenology, the main concept of this thesis, provides valuable information about climate change and biodiversity. It is the study of the timing of recurring biological events in the biosphere as well as of the causes of their timing (Lieth, 1974). The responses of ecosystems to climate variations can be examined with phenology metrics such as emergence of the first leaf, green-up, senescence and dormancy or on a more abstract level with the start of the growing season (SOS), end of the growing season (EOS) and length of the growing season (LOS). These events prove to be robust indicators for climate variations; phenology is therefore an emerging field of climate change science (Menzel et al., 2006; Cleland et al., 2007; Parmesan, 2007; Rodriguez-Galiano et al., 2015). Phenology is furthermore an indicator for biodiversity (Pereira et al., 2013; Skidmore et al., 2015) and useful to estimate carbon cycles (Goulden et al., 1996).

The studies of Fitzjarrald et al. (2001), Cleland et al. (2007), Parmesan (2007) and many others have shown that the changing climate has led to an earlier biological onset of spring and has delayed the beginning of biological winter over the last decades. The study of Garonna et al. (2016) examined the LOS over the last three decades with worldwide Normalized Difference Vegetation Index (NDVI) data and the results show an on-going trend of longer growing seasons. However, they also found areas with a trend of towards a shortening season length. Reasons for this may include changes in biodiversity and less precipitation in summer (Sweet et al., 2015; Garonna et al., 2016).

Phenology is sensitive to changes in biodiversity because different species have a different growing season length (GSL) and SOS and EOS. An example is the study of Sweet et al. (2015) in Alaska, which examined the phenology of deciduous shrubs and an evergreen graminoid area. The GSL of shrubs is shorter than the one of the graminoid area and since the abundance of shrubs has been increasing, land surface phenology (LSP) measurements show a negative trend of GSL. Vice versa, biodiversity is sensitive to changes in phenology. Ecological niches appear or vanish depending on the possible GSL.

Due to changes in temperature behaviour, snow melt and snow onset shift and thereby determine space for ecological niches.

The duration of the biological growing seasons is furthermore strongly connected to the photosynthesis rate of plants, primary productivity, the gas and water exchange of ecosystems and many other processes in the biosphere and atmosphere. The GSL is a key constraint on primary productivity, and therefore for the gross photosynthesis rate. Phenology metrics are consequently useful to estimate carbon cycles from a local to a global level (Goulden et al., 1996; Nemani et al., 2003; Richardson et al., 2007; Ahrends et al., 2008; Penuelas et al., 2009, Richardson et al., 2012).

1.2 Plant Phenology and Land Surface Phenology

Phenological measurements have been produced for centuries. In the beginning, farming families created time series of plant emergence, fruiting and harvest dates (Sparks and Menzel, 2002; Ahrends et al, 2008). The scientific community nowadays uses field, camera and satellite observations of phenology as an indicator for climate variations, biodiversity and carbon fluxes. For over three decades, satellite images have been providing a way to observe LSP on a global scale. However, the temporal and spatial resolution is limited, as well as the observation of single species (Menzel, 2002; Hufkens et al., 2012). In the recent decade, many plant phenology (PP) studies using consumer-grade cameras (phenocams) have emerged (e.g. Richardson et al., 2007; Ahrends et al., 2008; Sonnentag et al., 2012; Hufkens et al., 2012; Richardson et al., 2013; Klosterman et al., 2014; D'Odorico et al., 2015). With relatively inexpensive off-the-shelf cameras, different greenness indices can be extracted and provide a way to calculate phenology metrics from specific species at a high temporal resolution.

Nevertheless, assessing the relationship between changes in vegetation and measurements of LSP and PP remains a challenge (Hufkens et al., 2012). Satellites measure a combined signal from different plant species and are therefore not representative of smaller ecosystems or single species (White and Nemani, 2006). Near-surface PP on the other hand is difficult to extrapolate over large scales (Hufkens et al., 2012). Still, the two observation methods are complementary. Near-surface phenology is

often used as validation or calibration for satellite sensor data and conversely LSP to upscale PP (Menzel, 2002; Rodriguez-Galiano et al., 2015).

1.3 Research Problem and Challenges

So far, only a handful of studies have compared satellite data with phenocam data (e.g. Hufkens et al., 2012; Klosterman et al., 2014; Rodriguez-Galiano et al., 2015; Nijland et al., 2016; Baumann et al., 2017; Liu et al., 2017). Only the studies of Nijland et al. (2016) and Baumann et al. (2017) made use of high-resolution satellite data (Landsat imagery). The other studies used data from the Moderate-Resolution Imaging Spectroradiometer (MODIS) and Advanced Very High Resolution Radiometer (AVHRR) data with a pixel size between 250 metres and 1.1 kilometres (MODIS, 2017; NOAA, 2017). New options for comparing high-resolution satellite imagery with phenocam data emerged with the launch of Sentinel 2 in 2015. By merging Landsat-8 and Sentinel-2 images, the temporal resolution improves substantially, and the Sentinel-2 images with a spatial resolution of 10 metres (as compared to 30 metres of Landsat 8) allow observing phenology on the level of communities or even plant species.

Measuring the phenology of different species in a phenocam image or different pixels in a Sentinel-2 image allows measuring biodiversity and comparing PP and LSP not only quantitatively but also qualitatively. Qualitative differences can be the different field of view (FOV) of the sensors, the different viewing angle, observation of different species, the temporal and the spatial resolution or the different characteristics of the sensor.

A sensor with a low spatial resolution, for instance MODIS, measures one vegetation signal over an area of several hundreds of metres. This means that signals from plants with an earlier SOS merge with the ones with a later SOS. Just by analysing trends with MODIS data it is therefore complicated to determine whether differences in phenology metrics stem from changes in biodiversity or from climate variations.

Technically, sensors can only measure certain greenness indices from which phenology metrics are computed. SOS or EOS are thus mathematical definitions and are difficult to correlate to biological events of vegetation. With satellite or camera data, it is possible to detect the actual start of the greenness increase, as well as the peak of greenness, but in

most studies the SOS and EOS are simply defined as the day of maximum increase or the day at which 50 percent of the seasonal amplitude is reached. The relation between environmental processes at ecosystem level and the derived phenology metrics is still not well understood. For example, from phenology metrics it is not possible to detect the moment when an ecosystem turns from a carbon source to a carbon sink (Richardson, 2007). Also, the knowledge of the physical processes that initiate leaf onset and senescence is still limited (D'Odorico et al., 2015). That is why Baldocchi et al. (2005) and D'Odorico et al. (2015) suggest that observational approaches using phenocams be broadly established and validated at ecosystem level to get new insights about the ecological processes that determine the phenology metrics. Hufkens et al. (2012) and Nijland et al. (2016) furthermore suggest using high-resolution satellite imagery in order to account for small-scale differences among vegetation and to create a better comparability with phenocam data.

1.4 Motivation

New approaches are necessary to understand the influence of environmental processes at ecosystem level on the timing of phenological events derived from satellite and phenocam data. A quantitative and qualitative comparison between PP and LSP at known biodiversity test sites could yield new insights on differences in phenology metrics. Explaining differences between near-surface and satellite remote sensing data from an ecological point of view can help finding qualitative, individual reasons for these differences and therefore improve the comparability between the methods and facilitate extrapolation of PP to a larger scale.

1.5 Research Questions

Based on the theory, the research problems and the motivation in the introduction part, two blocks of research questions were defined. The first one covers the topic of PP, with the aim to find out whether biodiversity can be assessed from phenocams and the high-resolution satellite sensor of Sentinel 2. Subquestions treat the subject of the comparability of the near-surface and remotely-sensed data, as well as the stability and availability of the data.

1. Is it possible to measure plant phenology using phenocam and high-resolution satellite data?
    a. How well do the measurements from phenocam and high-resolution satellite data coincide?
    b. What influences does the data availability and stability have on the analysis?

The second block of research questions targets the comparison of PP and LSP. Is phenocam data able to validate phenology mapped with satellite data, and conversely, is it possible to extrapolate from point (phenocam) to area (biodiversity test sites)? Besides the comparison of the two paradigms PP and LSP, the two vegetation indices green chromatic coordinates (GCC) and NDVI are compared. Quantitative differences are shown and qualitative differences interpreted using factors like different vegetation species, ecological processes, the field of view (FOV) of the sensor, and sensitivities of the indices.

2. To what degree do the metrics derived from PP and LSP observations coincide?
    a. Which qualitative and quantitative differences can be described comparing the two paradigms?
    b. Which qualitative and quantitative differences occur comparing GCC and NDVI?

1.6 Structure of the Thesis

The analysed biodiversity test sites and the phenocam and satellite data used are introduced in chapter 2, followed by the methods in chapter 3. The results of the analysis are presented in chapter 4 and discussed in chapter 5. Finally, the conclusions complete the thesis in chapter 6.

2 Background and Data

This chapter gives an overview of the biodiversity test sites (Section 2.1) and the data (Section 2.2). To compare PP and LSP, data from phenocams (Section 2.3) and satellite sensors (Section 2.4) had to be acquired. The former stems from phenocams installed at the test sites, the latter from Google Earth Engine (GEE, Gorelick et al., 2017).

2.1 URPP Global Change and Biodiversity

Currently, the University of Zurich (UZH) has ten University Research Priority Programs (URPP), one of them is on Global Change and Biodiversity (GCB). As part of this URPP, six biodiversity test sites have been established in different climatic zones and on different latitudes, each of them with different levels of impacts of the five global drivers habitat change, climate change, invasive species, overexploitation and pollution (URPP GCB, 2017).

Figure 2.1: URPP biodiversity test sites (GEE).

2.2 Test Sites

The test sites Laegern, Kytalyk, Haibei, Aldabra and Borneo (Figure 2.1) are equipped with phenocams that record images every hour. The data from Borneo was not used, because the tropical rainforest region does not show clear seasonality (URPP GCB, 2016a). Phenocam images of Aldabra were processed initially, but did not lead to usable

results. The comparison between PP and LSP was therefore carried out for Laegern, Kytalyk and Haibei.

Laegern

The Laegern test site is located at 47.48N, 8.40E and the phenocam takes images of the mixed deciduous mountain forest (URPP GCB, 2016b). Thirteen different tree species grow in the test site area (Appendix: Table A-1). Sixteen regions of interest (ROIs, Figure 3.2) covering different tree species in the images were examined. Data from the phenocam is available since July 2015. 2016 was therefore the only year to work with, where data from a whole growing cycle was available (Table 2-1).

Figure 2.2: Phenocam images from Laegern test site from the first of February, May, August and November 2016 respectively.

Kytalyk

The test site is located in Siberia at 70.82N, 147.47E in the Kytalyk nature reserve (URPP GCB, 2016c). With grass and shrubs, at least two different tundra vegetation types can be discerned and analysed in the phenocam images. Data is available for 2015 and 2016 (Table 2-1). Unfortunately, the camera angle changed slightly on the 22 and 23 June 2016. The reference panel moved the most (about 30 percent of the FOV to the right), fortunately, the FOV of the camera did only change marginally. By drawing the regions of interest with enough margin, the shifts in the FOV did not change the vegetation species content of a ROI and the data could still be used.

Haibei

The test site on the Tibetan plateau is located at 37N, 101.21E and the vegetation type is alpine meadow (URPP GCB, 2016c). The analysed ROI consists of the whole image because it was not possible to define different vegetation types in the image. Phenocam

images were just available from the end of July to December 2015 and from January to the middle of June 2016. It was therefore only possible to analyse two halves of a growing season (Table 2-1).

Aldabra

Aldabra is a limestone atoll that is part of the Seychelles Islands. The subtropical climate has dry and wet seasons (URPP GCB, 2016d). Several changes in the camera angle made alignment of the images challenging. Furthermore, for a time span of two months the camera was looking vertically to the ground, which led to unusable images and thus a data gap.

2.3 Phenocam Data

Phenocams are consumer-grade digital cameras that are used to observe vegetation. Consumer-grade means, that the cameras were designed to reproduce the human vision and to be used in everyday life. Most phenocams thus have a red, blue and green channel and are not able to measure infrared which is typically used to monitor vegetation in remote sensing (Nijland et al., 2014). These off-the-shelf cameras provide a relatively inexpensive way to monitor phenology. The automated recording of pictures allows producing a continuous record of vegetation data at a high temporal resolution with little effort for years or even decades (Richardson et al., 2009; Brown et al., 2016). Furthermore, outliers or disturbances in the data can easily be visually inspected and causes (e.g. snowfall or fog) can be identified (Richardson et al., 2007).

On the other hand, phenocams are vulnerable to weather influences like lightning strikes or storms that change the camera angle or animals that damage the phenocam. Such disturbances can lead to data gaps if the installation is not monitored regularly (Richardson et al., 2013). Also, it might be difficult to find a FOV that is representative of the larger area (Rodriguez-Galiano et al., 2015). On the URPP GCB test sites however, the FOV was selected to represent the whole test site or even the regional vegetation system.

Figure 2.3: A phenocam overlooking vegetation (left) and the tower at Laegern test site mounted with two phenocams (right) (Flickr, 2011 & courtesy Bastian Buman).

The phenocam is usually installed on a tower or something similar that places the camera above the vegetation. In the northern hemisphere, it should furthermore point north to reduce lens flare, observation of shaded vegetation and forward scattering of vegetation (Richardson et al., 2013).

Phenocam images from the URPP biodiversity test sites are available from the beginning respectively middle of the year 2015. At the start of this thesis, only the years 2015 and 2016 were ready for the data analysis (Table 2-1).

Table 2-1: Temporal availability of phenocam data at the URPP GCB test sites.

	Laegern	**Haibei (Tibet)**	**Kytalyk (Siberia)**	**Aldabra**
Availability (Effective 9/2017)	07/2015-12/2016	07/2015-06/2016	01/2015-12/2016	01/2016-12/2016
Number of images (year)	3843 (2016)	3997 (2015-2016)	4582 (2015), 4300 (2016)	2018 (2016)

2.4 Satellite Data

Satellite data have provided a method to monitor phenology worldwide for over three decades. AVHRR data from National Oceanic and Atmospheric Administration (NOAA) satellites or MODIS aboard the National Aeronautics and Space Administration's (NASA) Terra and Aqua satellites have provided data at a moderate spatial resolution (1.1

kilometre and 500 metres respectively; NOAA, 2017; MODIS, 2017). NASA's Landsat-8 and ESA's Sentinel-2 satellites provide spectral data at much higher spatial resolution (30 m and 10-20 m respectively). Landsat-8 data is available since April 2013, Sentinel-2A data since the end of June 2015. The second Sentinel satellite (2B) was launched in March 2017 (ESA, 2018), thus for the years of interest 2015 and 2016 only data from Sentinel 2A could be used. Landsat 8 and Sentinel 2 were selected for their high spatial resolution and MODIS for its daily worldwide coverage since the year 2000. Beside the swath width of a satellite, the number of images available (Table A-3) is also dependent on the latitude. The temporal resolutions in Table A-2 are average numbers for the equator; more images are recorded with latitudinal distance. For Sentinel 2, only few images are available for the year 2015 because of its launch date in the middle of that year (23 June 2015). Sentinel-2 data was therefore only processed for 2016.

The Sentinel-2 (Level 1C) and Landsat-8 (Level 1T) data are both 'top of atmosphere' (TOA) products, which means that the data has not been corrected for the influences of the atmosphere. Because of their similarity, the two datasets could easily be merged together and a new dataset with more measurements could be created. The merged dataset (S2L8 in this thesis) allowed for a better temporal approximation of vegetation activity and more precise extraction of phenology metrics.

On the other hand, the MODIS data used has been processed to represent the 'bottom of atmosphere' or more specifically 'surface reflectance' (SR). In order to have comparable data for MODIS, the Landsat-8 surface reflectance product (L8SR) was downloaded and processed separately for the three test sites for 2016.

Google Earth Engine as data source

GEE is a platform that makes a broad catalogue of satellite imagery available to users and allows them to process the data in the GEE application programming interface (API).

The MODIS, Landsat-8 and Sentinel-2 products are freely available on GEE. Time series for a certain time span and in a certain ROI (point or area) can be created (Appendix E: GEE time series). In order to process the data more flexibly, the data was exported using PyCharm (JetBrains, 2017).

3 Methods

In this chapter, the process of deriving comparable phenology metrics from the available phenocam and satellite data is described. This includes extracting digital numbers (DNs), calculating indices, filtering the data, curve fitting and extracting phenology metrics (Figure 3.1).

The goal of processing the data was, to distinguish between different plant species when analysing ROIs in phenocam images and to compare the measurements from phenocam and satellite data. To do so, ROIs were defined manually and their content processed using statistical computing software.

3.1 Data Extraction

3.1.1 Phenocam Data

The phenocam data is available as common Red-Green-Blue (RGB) images in JPEG format. Because the phenocams at the URPP GCB test sites are not connected to the internet, the data has to be collected manually by the responsible researchers. Due to the difficult accessibility of some test sites, the data is being collected once or twice a year and is therefore available with a delay of up to one year (e.g. for Kytalyk).

The study of Richardson et al. (2009) found that the variation of SOS dates between the different sub regions in an image varied up to one week. In this study, as many vegetation groups as possible were analysed to detect such indicators of biodiversity. For that purpose, ROIs were defined within the phenocam image of the test site. Figure 3.2 shows all the defined ROIs at the respective test sites. Beside the smaller ROIs containing a single vegetation type, one big ROI per test site was defined to cover a large FOV that approaches the mixed pixel a high-resolution satellite sensor would see. This ROI is referred to as the ROI of the 'whole image'. Because of the slight change of the camera viewing angle in Kytalyk in 2016, different ROIs had to be drawn for the two years.

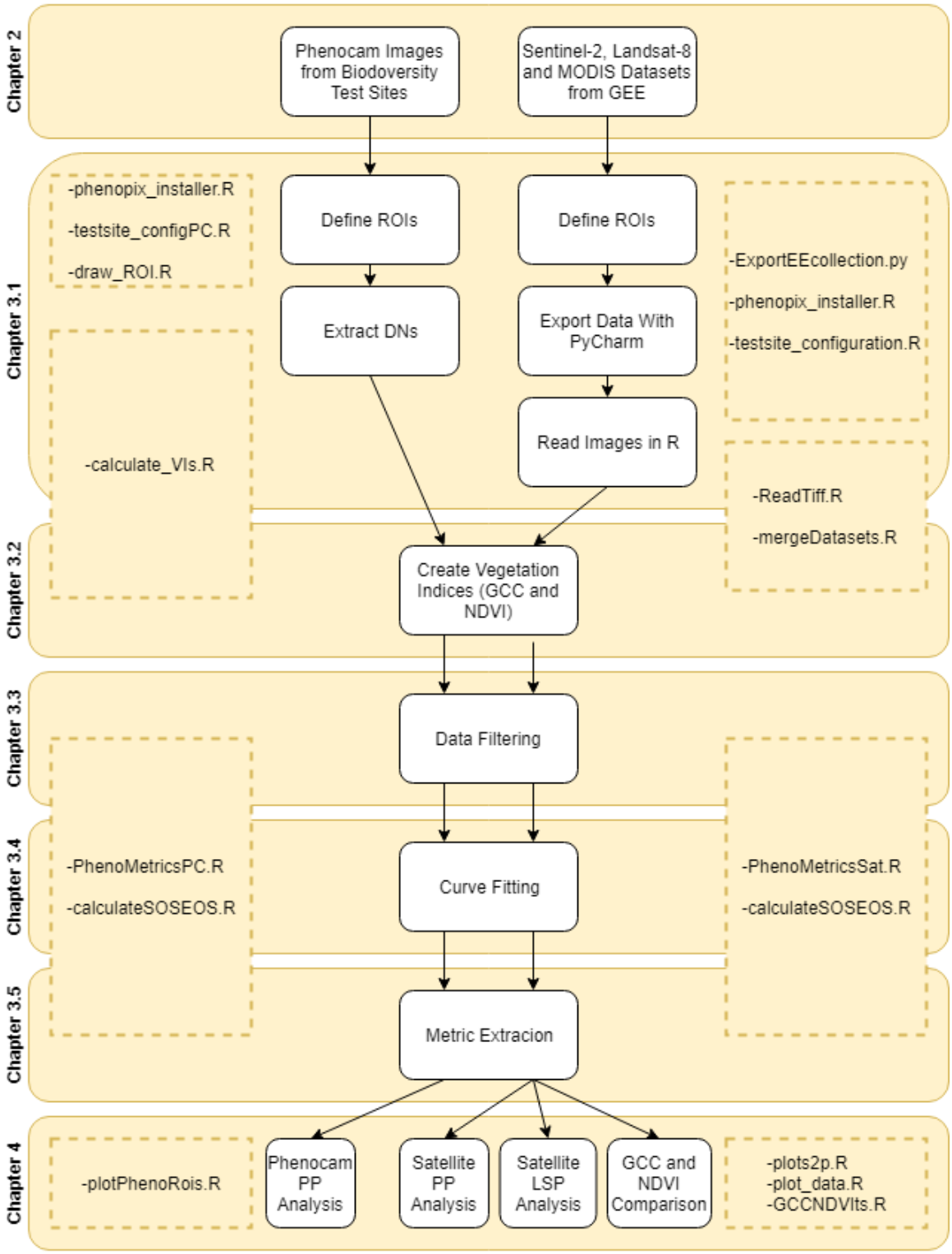

Figure 3.1: Working steps for the generation of phenology analysis of phenocam and satellite products. The boxes with dashed lines contain the filenames of the code used. The yellow polygons refer to the chapter of this thesis, the white polygons represent the working steps. Abbreviations: Google Earth Engine (GEE), region of interest (ROI), digital numbers (DNs), green chromatic coordinates (GCC), plant phenology (PP), land surface phenology (LSP).

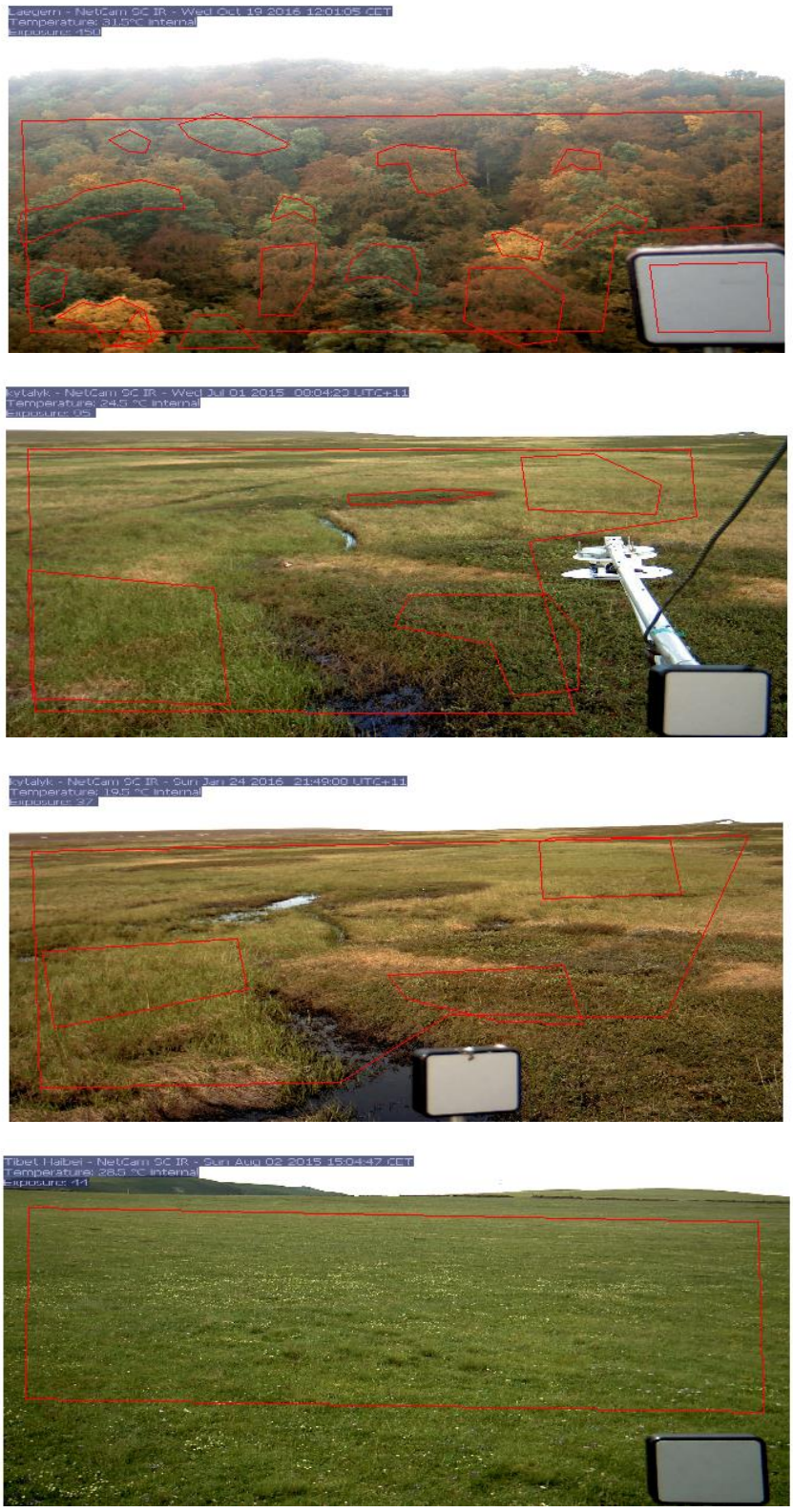

Figure 3.2: Examined regions of interest at the test sites Laegern (2016), Kytalyk (2015), Kytalyk (2016) and Haibei (2015/2016) (from top to bottom).

In a next step, the average DNs of the three camera channels red, blue and green were extracted over the series of the whole year from each ROI. Figure 3.3 shows the DNs of a ROI at Laegern test site over the year 2016. The DNs are typically measured between 0 and 255 and displayed over the course of one year. The data gaps in January and March stem from manually removed images with fog, snow or darkness (Section 3.1.2). The difference between the analysis with and without these images is evaluated in Section 4.2.

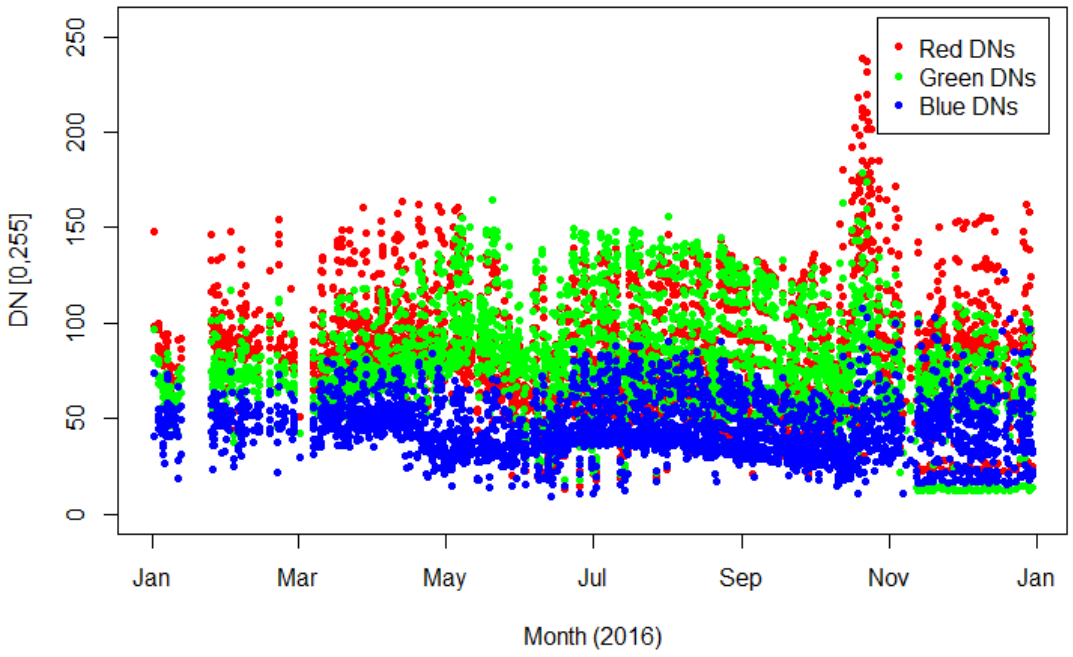

Figure 3.3: Red, green and blue digital numbers (DNs) of an examined tree at Laegern test site 2016.

The process of drawing ROIs and extracting the DNs over the whole time series of a ROI was conducted with the R package 'phenopix' (Filippa et al., 2016; R Development Core Team, 2008). This package provides functions to extract data from ROIs over a time series of a year as well as different filter, curve fitting, and metrics extraction methods.

3.1.2 Data Stability of Phenocams

The influence of different illumination conditions was evaluated for the Laegern test site with a ROI containing only the reference panel. Some studies (e.g. Richardson et al., 2009, Sonnentag et al., 2012, Richardson et al., 2013) already discussed the use of the reference panel and stated that it could be useful to correct for the day to day variation in

illumination, but that the values will still not be comparable across test sites because of the different cameras used.

Furthermore, to assess whether dark phenocam images, or fog and snow have a disturbing influence on the calculated vegetation index, these images were manually removed for the months January to July. Both datasets were processed and the differences compared in Section 4.2.

3.1.3 Satellite Data

GEE allows processing the available satellite data directly in the GEE-API. However, in this study the data was exported from GEE and processed with the exact same methods as the phenocam images. Exporting a single image in GEE is possible with an already implemented export function. Exporting series of images is more complicated but possible using the PyCharm-API.

3.1.3.1 Land Surface Phenology Analysis

The geographic extents of the satellite data were defined to represent an area containing the FOV of the phenocam. Figure 3.4 shows the polygon representing the extent of the satellite data at the Laegern test site (green), the position of the phenocam (red point) and the ROI defined for the pixel-wise analysis (red, Section 3.1.3.2). The green polygon has a size of 500 x 250 metres and the exported data consists of every satellite data pixel that falls within or overlaps with the polygon. This means that the exported data may stem from a larger area than defined by the polygon. This applies mainly for the MODIS data with a pixel size of 500 metres and to a smaller extent for the Sentinel-2 and Landsat-8 data. The four channels needed to calculate the GCC and NDVI (red, green, blue, and near infrared) were exported.

Figure 3.4: Laegern test site with the position of the phenocam (red point), the polygon for the land surface phenology analysis (green, 500 by 200 metres) and the polygon for the plant phenology analysis with Sentinel-2 data (red, 40 by 40 metres) (GEE).

Like for the phenocam data, the files were processed with R and the mean reflectance values within the polygon were used for calculating phenological metrics.

3.1.3.2 Plant Phenology Analysis

In a next step, the Sentinel-2 data was evaluated pixel-wise (instead of the polygon mean) in order to assess PP as closely as possible. The goal was to measure the signal of different plant species and to assess biodiversity as well as to compare the phenological variation among the different pixels with the variation between the different phenocam ROIs.

A smaller region of four by four Sentinel-2 pixels (i.e. 40 by 40 metres) in the FOV of the phenocam was selected for this purpose. Such an area approaches the extent for which individual trees – and thus species – can be distinguished in the phenocam imagery. As described in Section 3.1.3, the region containing these 16 pixels was exported, but instead of calculating the average of the values over the whole ROI, a loop to process every single pixel as an own ROI was created. Afterwards the same methods as for the other satellite products were applied (Sections 3.2 to 3.5).

3.2 Index Calculation

3.2.1 Phenocam Data

The values of the DNs show a relatively high variation over a single day. Reasons for that are mainly the different recording times involving different illumination strengths but

also weather effects like snow, rain, fog, clouds, sun or condensation on the camera lenses (Richardson et al., 2007). A vegetation index that is widely used for phenocam images (e.g. by Richardson et al., 2007; Sonnentag et al., 2012; Richardson et al., 2013; Klosterman et al., 2014 and Inoue et al., 2015) is the channel percentage, also known as chromatic coordinates (CC, Gillespie et al., 1987). CC normalise the data and show the ratio between one colour and the overall brightness. CC are calculated using Formula 1.

$$CC[colour\ x] = \frac{DN[colour\ x]}{DN[red]+DN[green]+DN[blue]} \quad (1)$$

The variation in brightness of the DNs can largely be suppressed by using CC (Richardson et al., 2013). Figure 3.5 shows the CC of the DNs in Figure 3.3. The ratio of the colours becomes visible, typical vegetation features like the higher greenness in summer and a maximum of red values in autumn are evident.

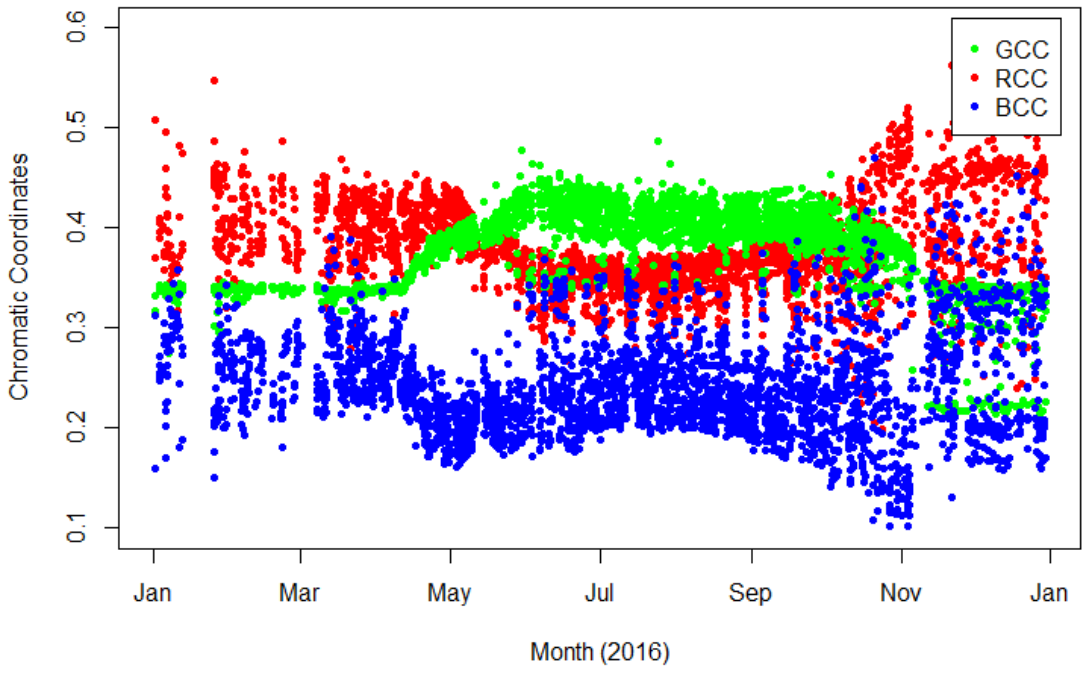

Figure 3.5: Green-, red-, and blue-chromatic coordinates (GCC, RCC, BCC) of a tree at Laegern test site 2016.

A similar index is Excess Green (ExGr), defined as follows (Woebbecke et al., 1995)

$$ExGr = 2 * DN[green] - (DN[red] + DN[blue]) \quad (2)$$

ExGr shows very similar green-up patterns like GCC (Richardson et al., 2007) but the latter was found to be more effective in accounting for different illumination conditions

(Sonnentag et al., 2012). This means that the difference in absolute brightness between summer and winter months with the summer months usually being brighter, is smaller when using CC. The authors further argue that the difference between different camera sensors (e.g. colour balance or bit depth) has a stronger influence than the values between the two indices and that CC and ExGr are therefore difficult to compare (Sonnentag et al., 2012).

Because of the marginal differences between the two indices and no advantageous benefits of ExGr, for this work, only CC were used to analyse the content of the datasets.

3.2.2 Satellite Data

In order to compare the satellite-derived data with the phenocam measurements, the same index had to be calculated. Using CC to monitor vegetation with satellite data is less common because of the strong sensitivity to atmospheric conditions. Instead, indices using the red-edge feature like the NDVI are more widespread (e.g. Hufkens et al., 2012; Klosterman et al., 2014; Nijland et al., 2014; D'Odorico et al., 2015; Garonna et al., 2016). For that reason, both GCC and NDVI were calculated for the satellite data. This allows a comparison between phenocam and satellite data as well as between the CC and NDVI.

The NDVI is defined as (Tucker, 1979)

$$NDVI = \frac{NIR-red}{NIR+red} \tag{3}$$

The advantage of the NDVI is, that is measures not only colour and brightness of vegetation but is also sensitive for the degree of vegetation activity and is not prone to the correlation that exists between the RGB bands. Tests to mount phenocams with infrared filters have been made (e.g. by Nijland et al., 2014), but the authors concluded that the conventional RGB images outperformed the infrared images due to issues with radiometric calibration.

3.3 Data Filtering

3.3.1 Phenocam Data

The CC (Figure 3.5) still show a diurnal variation, mainly responsible for that are the different illumination conditions on overcast and sunny days, disturbances of rain, snow,

fog, white frost or dew and still marginally the acquisition time, season or the solar altitude (Sonnentag et al., 2012; Richardson et al., 2013). Images with disturbances tend to have lower GCC values, because neither darkness nor snow or fog makes the ROI greener (Section 4.2). To account for these effects, Sonnentag et al. (2012) propose a maximum-filter approach with a three-day moving window that uses the greenness values at the 90th percentile. The moving window collects all greenness values over a period of three days and assigns the value of the 90th percentile to the middle day of the three. After filtering the data with this method, one value every third day is left. To filter the phenocam data of this project, the method of Sonnentag et al. (2012) was adjusted, so that a value for every single day is calculated, consisting of the 90th percentile of a three-day window.

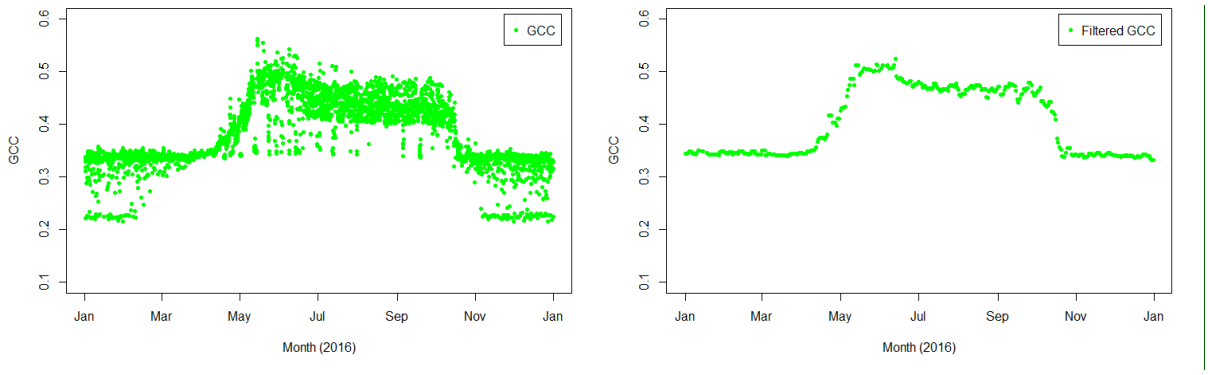

Figure 3.6: Green Chromatic Coordinates (GCC) of Laegern test site (left) and maximum-filtered data (three-day moving window and 90th percentile value).

Figure 3.6 shows the maximum-filtered GCC values for the ROI at the Laegern test site. The data resemble a typical phenology curve and are corrected for disturbances and illumination effects and therefore useful to calculate phenology metrics.

3.3.2 Satellite Data

Disturbances in the satellite data stem mainly from clouds. There is no diurnal variation of brightness because the images are always recorded at the same time. A seasonal variation remains due to the changing sun angle. The disturbances of clouds can be assumed to always lead to a less green image or to lower NDVI values because clouds tend to have a lower NDVI value due to a bright reflection in the red and a low reflection in the infrared range (Tang and Oki, 2007). Therefore, the maximum-filter is also suitable

for the satellite data. The same filtering method as for the phenocam data was used, whereby the moving window collected the values of three consecutive measurements. As a consequence, the moving window may have taken values from a much longer time period, because Landsat-8 and Sentinel-2 data have had sparser measurements. The size of the moving window was adjusted to five days for the MODIS data since the daily availability of images allowed this. Figure 3.7 shows the maximum-filtered GCC data (green) from the Sentinel-2 images at the Laegern test site plus all the GCC measurements (black). Cloud cover on at least three consecutive measurements lead to very low GCC values in June and August. To interpolate such gaps, as well as to extract metrics from the filtered data, a curve had to be fitted to the data.

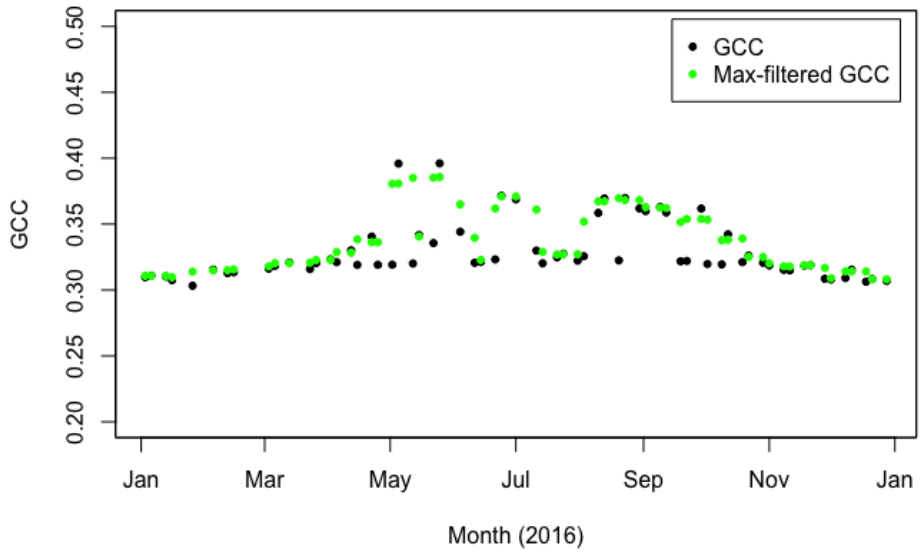

Figure 3.7: Sentinel-2 green chromatic coordinates (GCC) data at Laegern test site (black) and the maximum-filtered data (green).

3.4 Curve Fitting

To extract phenology metrics like SOS and EOS, a curve had to be fitted to the filtered data. A fitted curve allows interpolating data and assigning a distinct value for the phenology metrics. The phenopix package provides already implemented curve fitting methods such as 'spline fit' or double logistic functions like the 'Beck fit', 'Elmore fit', 'Klosterman fit' and 'Gu fit' (Beck et al., 2006; Elmore et al., 2012; Klosterman et al., 2014; Gu et al., 2009 respectively, Filippa et al., 2016).

Filippa et al. (2016) recommend using a double logistic function instead of a spline fit as long as the fits are anyway similar, as the former are more robust. Furthermore, most of the recent studies on phenology with remote sensing data used logistic models (e.g. Fisher et al., 2006; Richardson et al., 2006; Richardson, 2007; Richardson et al., 2009; Schwartz and Hanes, 2010; Zhang et al., 2003; Hufkens et al., 2012). In their study, Klosterman et al. (2014) assessed different fits (cubic spline and three simple sigmoid fits) including their own method with the root mean square error (RMSE).

The decision on which fitting method to use for this thesis was made after assessing the three criteria success of fitting a curve to the data, the RSME and how much sense the fitted curve made modelling vegetation activity. Not every method could be applied to every sensor and test site. Therefore, the aim was to use the same fitting method for at least a vegetation index of the same sensor (e.g. all the GCC data of Landsat 8 was fitted with a Beck fit, Table A-4).

Figure 3.8 shows examples of the different fits for the filtered datasets: Laegern Landsat-8 GCC (left), Haibei Landsat-8 NDVI (left middle), Haibei Sentinel-2 NDVI (right middle) and Laegern Phenocam GCC. The provided algorithms did not always provide a suitable fit, e.g. the spline fit is not meaningful in any of the first three examples and the Klosterman fit does not work for the dataset in the first column. In these cases the respective RMSEs are not significant either.

The second column in Figure 3.8 containing the Landsat-8 NDVI data from Haibei gives an example for the (second) criteria RMSE. After testing all curve fits for Landsat-8 data over all test sites and years, only the Klosterman and the Beck fit have been shortlisted. Finally, the Beck fit was chosen for its lower RMSE.

The same two fitting methods were the only options for the Sentinel-2 NDVI data (example from Haibei in the third column). Here the choice fell on the Beck fit, because the curve modeles the vegetation activity better than the Klosterman curve. Whereas the former is closer to the maximum values, the latter does not reach the maximum values because of lower values that drag the curve down. It is assumed that these lower values

stem from cloud cover and that therefore the maximum values represent vegetation. For that reason the Beck fit was chosen despite the higher RMSE (third criteria).

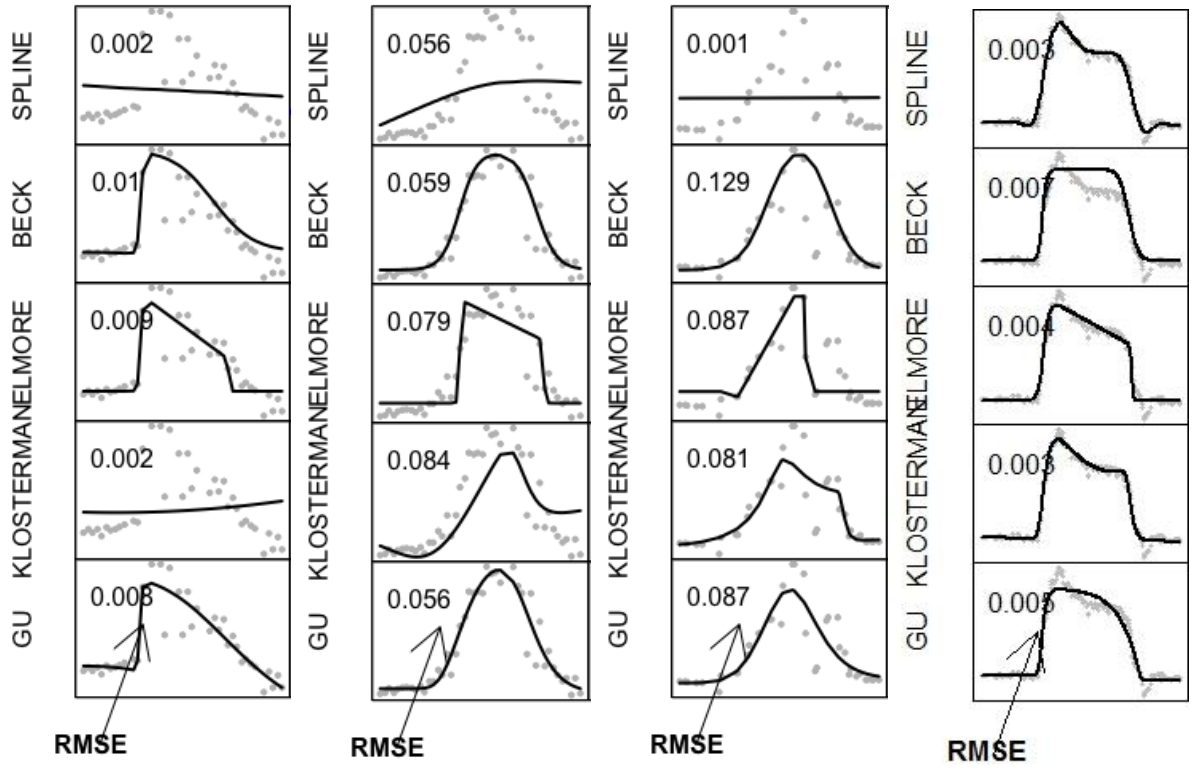

Figure 3.8: Different fitting methods (Spline, Beck, Elmore, Klosterman and Gu) for the filtered Laegern Landsat-8 green chromatic coordinate (GCC) data (left), Haibei Landsat-8 NDVI data (left middle), Haibei Sentinel-2 NDVI data (right middle) and Laegern Phenocam GCC data (right). The number indicates the RMSE. Certain methods were not able to generate a suitable fit due to issues with the algorithm, in these cases the RMSE is not significant.

Table A-4 summarises the chosen fitting methods per dataset and vegetation index. For the S2L8 NDVI and the L8SR products, different fitting methods had to be chosen depending on the test site.

The lowest RMSE and the best fit for the phenocam data was reached with the spline fit method (fourth column of Figure 3.8). As the phenocam datasets provide much more data points than the satellite datasets and because of less disturbances between vegetation and the sensor (e.g. clouds, fog), the filtered data had already a very small variation and allowed the spline function to be very accurate.

3.5 Metrics Extraction

The most common phenology metrics extraction methods are derivatives and thresholds. For the former, the SOS and EOS are assigned to the maximum increase respectively decrease of the curve or the highest curvature change rate. These metrics are computed with the first respectively second derivative of the curve. Using thresholds to assign values to the metrics was the more appropriate way for this work, especially because different fitting methods were used. A threshold is usually set at 50 percent between the maximum and the minimum value of the curve. The first day over this threshold is taken as the SOS and the first day after the last time the curve was over the threshold as the EOS. However, this method is not always robust if the curve crosses the threshold more than twice due to outliers. Figure 3.9 shows phenology metrics derived by the implemented phenopix functions 'threshold (trs)' and 'derivatives' and problems that can occur. In the first row, the phenopix threshold method defines the EOS only a couple of days after the SOS, because the curve crosses the 50-percent threshold again. To account for this problem, two other functions were developed. One function takes the longest consecutive part over 50 percent as the growing season and the other one assigns the first value over 50 % to the SOS and the first value after the last time the curve was over 50 % to the EOS. The first function had to be applied on data like the one in the second row of Figure 3.9 and the second function on data like in the first row. Deciding which of the different threshold functions to take was done manually after analysing the fitted curve.

An issue with the derivatives method can be recognised in the second row on the right of Figure 3.9. The SOS is assigned to the maximum increasing part of the curve, but due to an outlier at the end of the year, this value is not representative of the actual SOS.

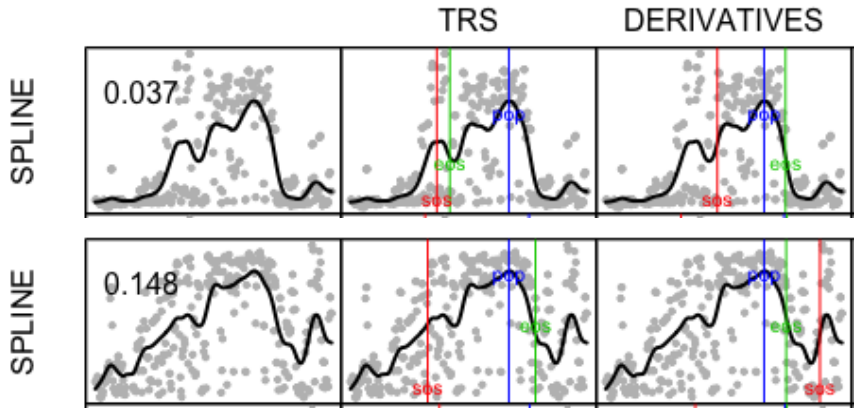

Figure 3.9: Spline fit for the Laegern green chromatic coordinate (GCC) (top) and NDVI (bottom) data 2016 with extracted phenology metrics (middle: 50% threshold (TRS), right: maximum increase/decrease (derivatives)) SOS (red), EOS (green) and peak of season (blue).

3.6 Comparison of GCC and NDVI

In order to compare the phenocam and satellite-derived GCC data with the NDVI data, the differences between the two indices had to be assessed quantitatively as well as qualitatively.

The study of Keenan et al. (2014: supplementary information) analysed the relation between satellite-derived GCC and NDVI data and ground observations (budburst for spring and leave colour change in autumn). They found an earlier SOS and a later EOS for the NDVI measurements and a later SOS and earlier EOS for the GCC measurements compared to the ground observations when using a spline fit. When using a logistic fit however, the NDVI values led to a later SOS compared to the ground measurements. Hufkens et al. (2012) compared metrics derived from ExGr, which is used almost identically to GCC (Richardson et al., 2007; Sonnentag et al., 2012; Inoue et al., 2015) and NDVI and found an earlier SOS but also an earlier EOS for the NDVI-derived metrics. Klosterman et al. (2014) on the other hand found that measurements from remotely-sensed data led to a later SOS and EOS, but they also remarked that the GCC data from satellite measurements was noisy, an issue that found support by Brown et al. (2016). The study of Walther et al. (2016) assessed the differences and relations between greenness, and photosynthetic activity. They found that the green-up lags behind the beginning of photosynthetic activity and that this effect is stronger on high latitudes.

Furthermore, they found that NDVI MODIS data generated an earlier SOS and later EOS than the greenness indices and that greenness generally shows a shorter season length than photosynthesis. For coniferous species, the photosynthesis lasts shorter than the greenness. As the NDVI is more sensitive to photosynthesis than GCC, it can be assumed that NDVI data should lead to longer seasons than GCC data for the deciduous forest and grasslands in Kytalyk and Haibei.

Since the comparison of metrics derived from the two indices depends highly on the processing methods, the test site and the instruments used, an own assessment for the three test sites with the same filtering, fitting and extraction methods as the ones in the main analysis was conducted. A MODIS time series between 2000 and 2016 was analysed, extracting phenology metrics for the NDVI and the GCC data. The goal was to find out, whether phenology metrics of one index can be expected to be systematically earlier or later than the ones of the other index as well as to detect a possible correlation between the metrics from the two indices.

4 Results

The observation of PP and LSP with focus on biodiversity, data stability, the correspondence between metrics derived from near-surface and remotely-sensed data and the comparison of the vegetation indices GCC and NDVI led to revealing results. In the first part of this chapter, phenology on species level (PP) is presented and analysed with near-surface measurements from phenocams and remotely-sensed data from Sentinel 2. The second part presents phenology from an ecosystem or test site level (LSP) and sets the results in relation to the PP measurements and compares the quantitative differences between the two used vegetation indices, GCC and NDVI.

Examinations were made for the temperate mixed forest at Laegern test site and the tundra in Kytalyk. For both sites, a continuous record of data with the possibility to discern between different vegetation types was available. Data gaps of phenocam images from Haibei and Aldabra test sites, however, made it difficult to model vegetation activity at these test sites. Beside the data gap in the Aldabra data in April and May, the factor mainly responsible for the amplitude in the vegetation indices was image quality rather than vegetation activity. The images were blurry and darker in the second half of the year. Because it was not possible to discern a green-up, the decision was made not to conduct an analysis for this test site.

Besides the presented graphs and tables (Figure 4.1 to Figure 4.4, Table 4-1), results that are referred to in this chapter can be followed up on in the Appendix (Figure B.1 to Figure D.8 and Table A-1 to Table D-7).

4.1 Observations of Plant Phenology

The examination of different plant species in the phenocam images showed revealing differences in vegetation activity concerning not only the SOS and EOS but also different green-up speeds, different magnitudes of GCC and different peaks of greenness. Both the near-surface measurements with the phenocam and the remotely-sensed data of Sentinel 2 allowed assessing biodiversity and measuring characteristics of different vegetation species.

4.1.1 Plant Phenology from a Near-Surface Perspective

The observations of the mixed deciduous forest at Laegern and the tundra in Kytalyk allowed distinguishing between up to thirteen different tree species in sixteen ROIs for the former test site and between the two vegetation types 'grass' and 'shrubs' in five ROIs for the latter test site.

The GCC representing the different species at Laegern test site showed a small variation in the phase where vegetation is not active. The green-up started at different times and with different speeds. The 50-percent threshold was reached between DOY 110 and DOY 125. For the whole image this was at DOY 113 (Figure 4.1, Table 4-1). During the growing season, the variation of the different greenness values was rather high and among the EOS dates the variation was much broader than for the SOS (DOY 251 to 307, DOY 278 for the whole image).

The analysed vegetation at the Kytalyk test site in 2015 also showed different green-up speeds, greenness levels and phenology metrics in summer during the growing season. The SOS varied between DOY 172 and 179 (178 for the whole image) and the EOS between DOY 231 and 234. In the phenocam image distinguishing between shrubs and grass was possible. The ROIs with shrubs had an earlier SOS (DOY 172 and 175) and EOS (231 and 232) than the ROIs containing grass (SOS DOY 177 and 179, EOS DOY 134). The SOS estimate for the whole image was – as anticipated – between the values of grass and shrubs (Table 4-1, Appendix B: Table B-5, Figure B.1).

Vegetation activity in 2016 was generally very similar to 2015 with the only difference being an overall earlier SOS for 2016 (DOY 171). The SOS and EOS lay within a range of four (DOY 169 to 172) respectively three (DOY 233 to 235) days. For 2016, it was not possible to recognise differences between shrubs and grass. The differentiation between the two vegetation types was difficult because only one ROI containing shrubs could be analysed (Section 3.1.1).

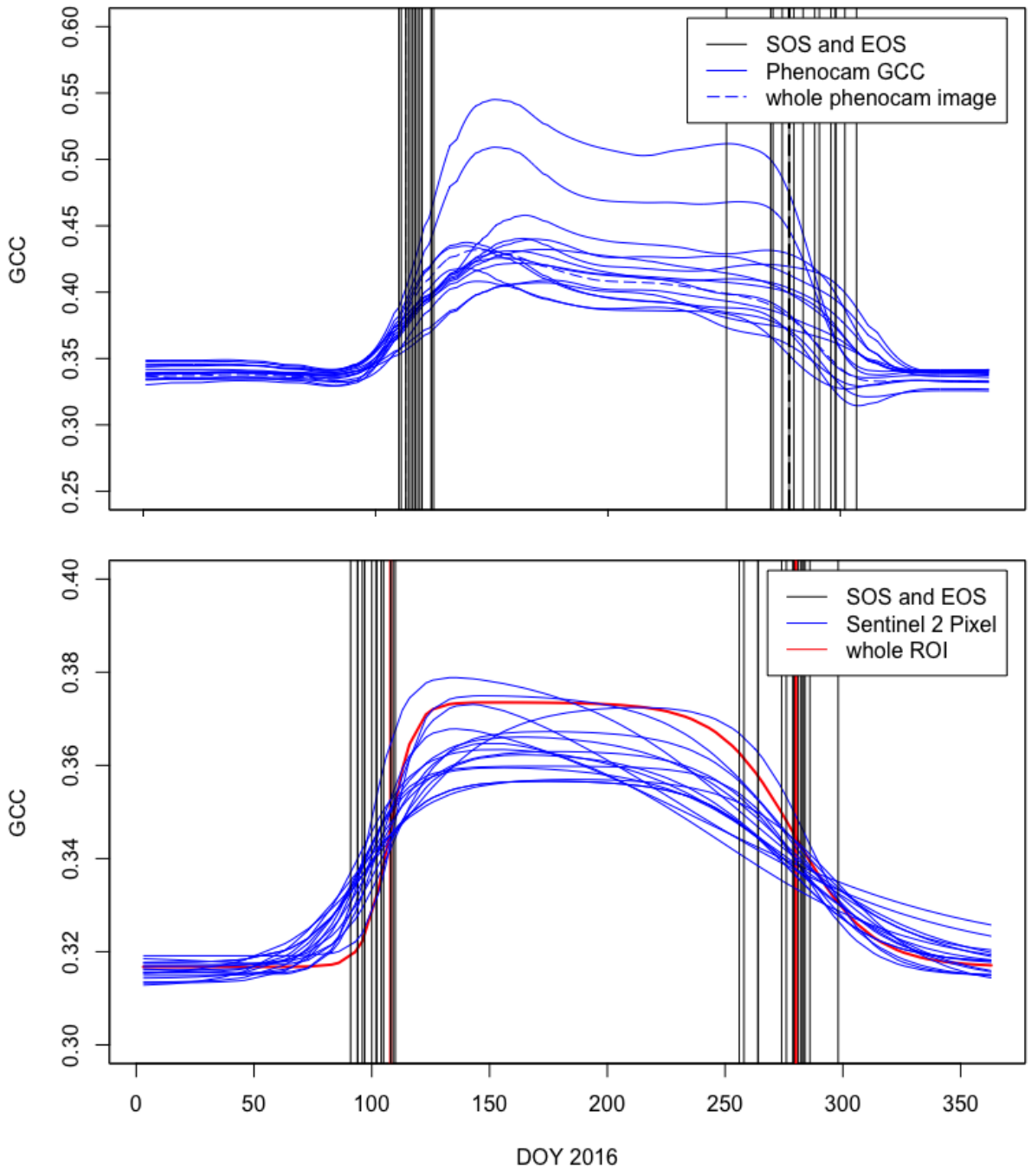

Figure 4.1: Phenology curves of sixteen regions of interest (ROIs) at Laegern test site 2016 with respective SOS and EOS as vertical lines from phenocam data (top) and Sentinel-2 data (bottom). Upper graph: The dashed line represents the data from the ROI containing the whole phenocam image and should by design be somewhere in the middle of the other curves as the data consists of all the other ROIs. It is expected that the ROI of the whole image approximates to what a satellite measures, as it merges the signals of the smaller ROIs and vegetation species, similarly to the signal a satellite sensor measures.
Lower graph: Phenology curves of sixteen Sentinel-2 pixels in the FOV of the phenocam at the Laegern test site. The red graph represents the Sentinel-2 dataset of the whole test site.

Table 4-1: Meta-analysis of plant phenology observations from phenocam and Sentinel 2. The range, mean and standard deviation (Stdev) of the examined region of interests (Phenocam) and the 16 pixels (Sentinel 2) are shown as day of year (DOY).

		Start of Season (DOY)					End of Season (DOY)				
		Min	**Max**	**Mean**	**Range**	**Stdev**	**Min**	**Max**	**Mean**	**Range**	**Stdev**
Near-surface (Phenocam)	**Laegern**	110	125	117.07	15	4.58	251	307	284.53	56	14.33
	Kytalyk 2015	172	179	176.20	7	2.77	231	234	232.80	3	1.30
	Kytalyk 2016	169	172	170.50	3	1.29	233	235	234.00	2	1.15
Remotely-sensed GCC 2016 (Sentinel 2)	**Laegern**	91	110	100.13	19	5.99	256	298	276.67	42	11.15
	Haibei	160	170	164	10	2.36	260	269	263.73	9	2.42
Remotely-sensed NDVI 2016 (Sentinel 2)	**Laegern**	108	122	113.67	14	6.02	285	312	297.07	27	8.43
	Kytalyk	158	173	165.73	15	4.81	257	261	258.80	4	1.17
	Haibei	152	156	153.40	4	1.03	286	291	287.93	5	1.71

4.1.2 Plant Phenology from the Remote Perspective of Sentinel 2

The analysis of PP at the test sites with remotely-sensed data revealed, similarly to the near-surface measurements, a significant variation of vegetation activity. The sixteen Sentinel-2 pixels within the FOV of the phenocam were the best possible approach to measure PP and to compare it to the near-surface measurements (Figure 4.1, Table 4-1).

The detected variation in vegetation activity of the mixed deciduous forest is again smaller for the SOS than for the EOS (19 and 42 days respectively). The Sentinel-2 data furthermore allowed analysing PP with NDVI instead of GCC. A similar variation of 19 days for the SOS and a shorter one of 28 days for the EOS was detected (Table 4-1).

In Kytalyk, the variation of vegetation activity revealed a different picture. The vegetation activity increased with different speeds and led to a variation of sixteen days among the SOS dates, whereas the decrease of vegetation activity proceeded simultaneously and led to a small variation of four days (Table 4-1). Furthermore, two groups of curves are distinguishable, one with a slightly faster green-up and lower maximum NDVI values, and a second group with a longer green-up period and marginally higher maximum values.

The analysis of PP was carried out with NDVI data because the low green reflection values of TOA products on high latitudes led to GCC values with an amplitude of only 0.02 and no distinct green-up was recognisable.

4.2 Data Stability of Phenocams

The additional ROI containing the reference panel at the Laegern test site was examined with the aim to check whether absolute brightness had an influence on the data. The results (Figure 4.2) show that the GCC remain very stable during the course of the year at a value around 0.335. Only the images without or with limited daylight (due to clouds or fog) led to lower values.

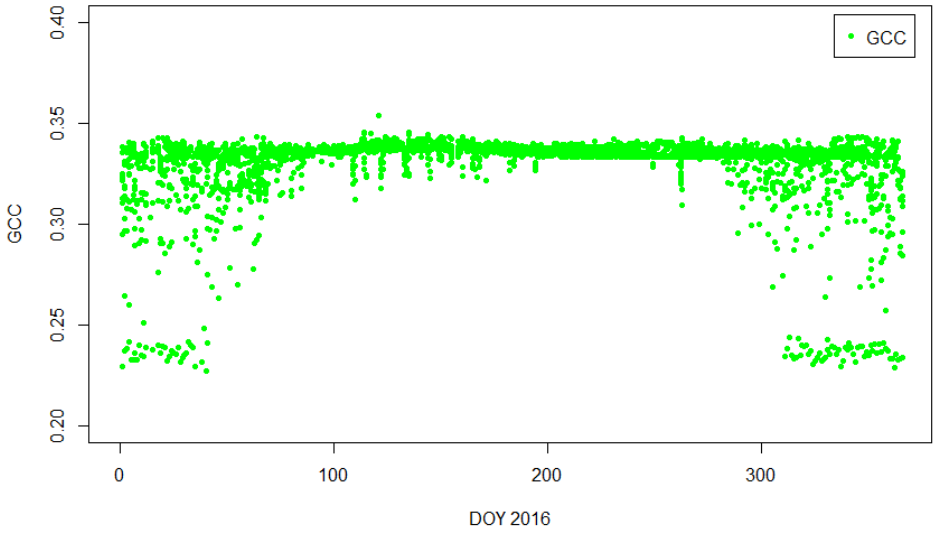

Figure 4.2: Green chromatic coordinates (GCC) for the reference panel at Laegern test site 2016.

To analyse whether illumination and weather influences limit the observation of vegetation activity, a second analysis was conducted. For the months January to July, every image that did not show vegetation due to disturbances of fog, snow cover or darkness (images taken before sunrise and after sunset) was manually removed from the dataset. As the maximum GCC values were not affected by removing these images, the process was not continued for the second half of the year and the other test sites. GCC values of dark images are the ones with the values around 0.22 of the days of year (DOYs) 0 to 40 as well as DOYs 310 to 365. Fog and snow cover lead to GCC values between 0.25

and 0.35 (Figure 4.3). The maximum-filter is therefore suitable to account for disturbances that affect the illumination or distort the measured colour of the vegetation.

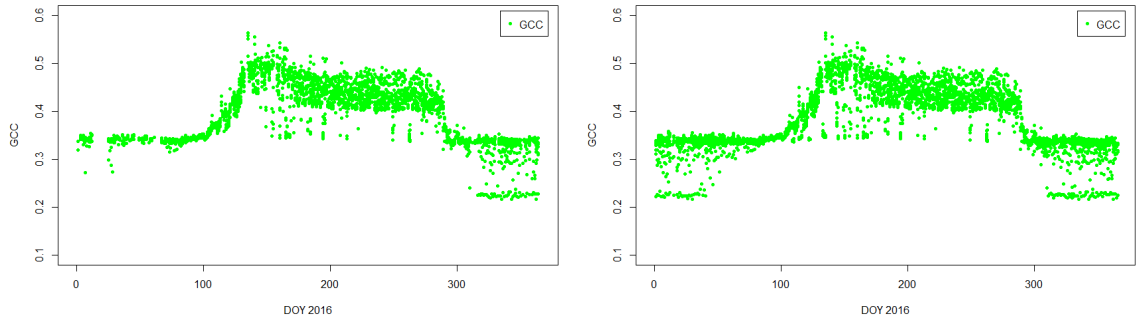

Figure 4.3: Green chromatic coordinates (GCC) of a ROI at Laegern test site 2016 without images of darkness, snow and fog between January and July (left) and with every image taken (right).

4.3 Observations of LSP

The LSP perspective allows observing regional ecological processes and analysing the vegetation activity of a small ecosystem or, in this case, of the biodiversity test sites. Instead of a distinction between vegetation species, the observation analyses the response of a merged signal of the whole area. In the first part, PP and LSP measurements are compared in order to assess whether PP can be used to validate LSP measurements and conversely whether PP can be extrapolated using LSP measurements. The second part evaluates the relation between the vegetation indices GCC and NDVI.

4.3.1 Comparison of PP and LSP

To find out whether the phenological activity of a single plant species is representative of the whole area around it, the LSP measurements had to be compared to the range of the PP signals. Comprehensive results presented in this section can be followed up on in Figure 4.4 and Appendix C.

The most successful comparison was the one using the same instrument for PP and LSP observations. In this case, the analysis with Sentinel-2 data. The observation of small regions with an area of 10 by 10 metres was compared to the area of the whole test site, with a size of 200 by 500 metres for the mixed deciduous forest and the alpine meadow, and 1 by 2 kilometres for the tundra test site.

The LSP metrics (whole ROI) from Laegern and Kytalyk test sites lay within the variation of the PP measurements for both the GCC and NDVI analysis. The analysis at the Tibetan test site revealed a different picture. LSP measurements detected a later green-up, marginally lower GCC values and an earlier EOS when analysing the GCC data.

The differences between the near-surface measurements of single vegetation species and LSP measurements with satellite sensors, however, were more pronounced. At Laegern (Figure 4.4, Table B-5), the Sentinel-2 and Landsat-8 data coincided very strongly for the SOS (DOY 106-108). MODIS detected a later SOS (DOY 119) and the SOS of the phenocam images (DOY 113) lay in-between the two. The SOS from the NDVI data was earlier than from GCC, except for the Sentinel-2 data. The EOS of the phenocam data (DOY 278) coincided very well with Sentinel 2 and MODIS (DOY 280 and 278 respectively). The merging of Landsat-8 and Sentinel-2 data led to an improved dataset with the same EOS as the phenocam and the MODIS data (DOY 278). The EOS derived from NDVI values was generally later than for the GCC values (except for MODIS one day before) and was very close to the phenocam measurement for Landsat 8 and MODIS (DOY 279 and 277 respectively) and a bit later for the merged S2L8 dataset (DOY 287).

For the SOS, the LSP metrics coincided better with the range of remotely-sensed PP measurements than the range of the near-surface measurements that lay later. Only SOS dates of MODIS GCC and Sentinel-2 and S2L8 NDVI measurements lay in this range. The EOS dates of both phenocam and Sentinel-2 data covered about the same ranges of DOYs which included all LSP metrics except the SR dataset from Landsat 8.

In Kytalyk, measurements of LSP revealed a longer growing season than the PP data from the phenocam for the years 2015 and 2016, excluding the Sentinel-2 data. The season length in 2015 calculated from MODIS GCC data was longer than the one calculated from the ground data (SOS: -12 days, EOS +9 days) and again longer from MODIS NDVI data (SOS: -15 days, EOS: +29 days).

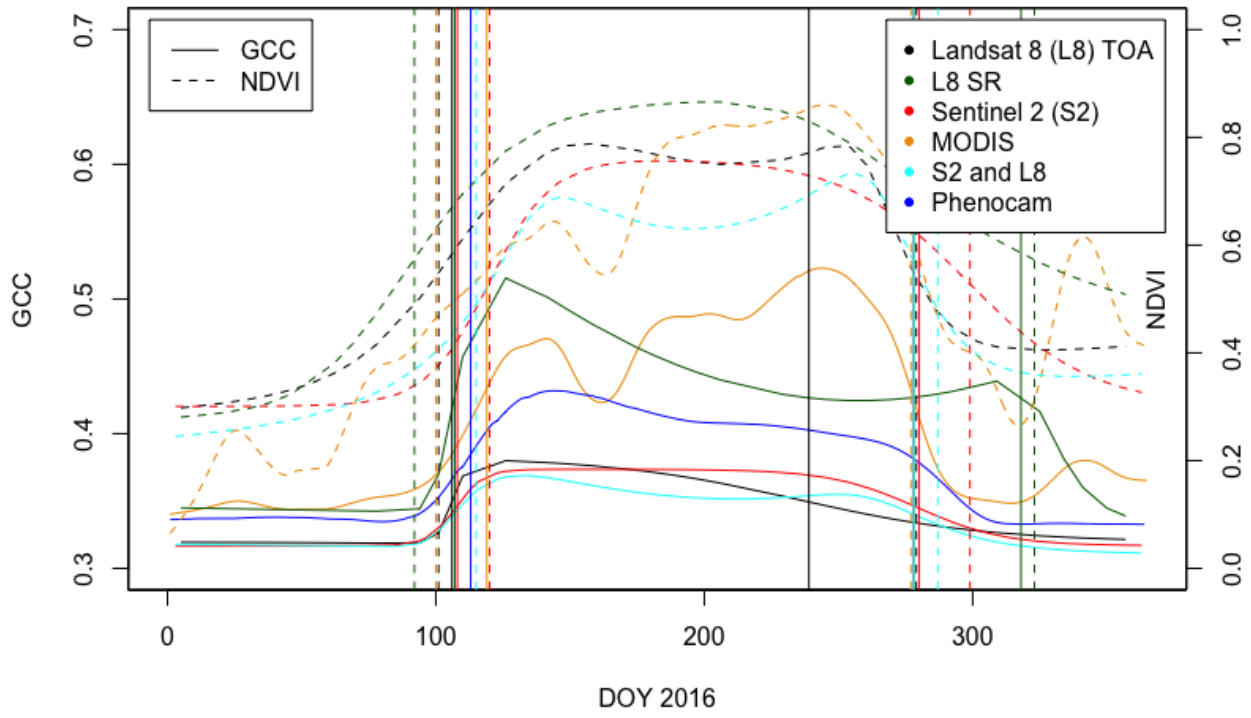

Figure 4.4: Phenology curves from the satellite and phenocam datasets for Laegern 2016. Both Landsat top of atmosphere (TOA) and surface reflectance (SR) data was used. The Sentinel-2 data represents also TOA values, MODIS data is processed to model SR. The dashed lines stand for the NDVI data, the solid line for the green chromatic coordinate (GCC) data. The vertical lines represent the start of season and end of season, calculated with the 50-percent value of the amplitude.

In 2016, the phenology metrics calculated from Sentinel 2, MODIS, L8SR and S2L8 coincided much better with the near-surface measurements from the phenocam (SOS: DOY 171, EOS: DOY 235). This was mainly due to the earlier SOS of the phenocam data, compared to 2015 (-8 days). MODIS also detected an earlier SOS, but only one and two days for GCC and NDVI measurements respectively. The SOS dates derived from the satellite GCC data varied between DOYs 162 and 180 and the EOS dates varied between DOYs 232 and 245. The season lengths calculated from NDVI data were longer yet again. For every dataset the SOS was earlier and the EOS later than the ones from the GCC data.

4.3.2 Comparison of GCC and NDVI Measurements

The results of the comparison of MODIS GCC and NDVI data showed unambiguously, that the 50-percent threshold was reached earlier for the SOS and lasted longer for the EOS of the NDVI data. Comprehensive figures, regression analyses and tables referred to in this section can be followed up on in Appendix D (Figure D.7, Figure D.8 and Table D-7).

In addition, the regression offered insights on the correlation between the metrics of the two indices GCC and NDVI. A correlation could only be detected for the Kytalyk test site (R^2 of 0.66 and 0.49 for SOS and EOS respectively) and the SOS at Haibei test site (R^2 of 0.44).

The correlation analysis of the pixel-wise processed data only showed a correlation between the metrics of the two indices for the EOS of Kytalyk and Haibei (R^2 of 0.36 and 0.33 respectively). Furthermore, at the Laegern test site the GCC data led to an earlier SOS and EOS. The season length was shorter for GCC at Haibei test site than the season length analysed with NDVI data whereas the Kytalyk GCC data was not suitable for comparison. Unlike for the MODIS time series, Sentinel 2 did not distinctly discover an earlier SOS for NDVI data. The EOS, however, was still detected to be later for NDVI data than for GCC data over all analyses (S2, S2L8, pixel-wise).

The phenocam-derived GCC measurements showed a later SOS and earlier EOS than the NDVI measurements of the different satellite sensors for both years at Kytalyk test site and the Laegern analysis in 2016. The only exception from the deciduous forest was the Sentinel-2 derived NDVI data (S2 and S2L8) with a later SOS and the MODIS and Landsat-8 data with the same EOS as the phenocam measurements.

5 Discussion

The results presented in chapter 4 are discussed and compared in the following chapter and set into the context of the research questions. In line with the first research question, the first part focuses on PP and the data stability of phenocams. To discuss the second research question, the two paradigms PP and LSP are compared with a focus on qualitative differences and the differences between GCC and NDVI are critically assessed.

5.1 Plant Phenology from a Near-Surface and Remote Sensing Perspective

The analysis of vegetation activity of single species (phenocam) or the area of small canopies (pixel analysis with Sentinel 2) has revealed a significant variation in SOS dates and an even broader variation for the EOS at the deciduous forest test site. The variation during the green-up is an informative indicator for biodiversity. Reasons for the broader variation concerning the EOS are manifold. Depending on the species, the leaves turn red earlier, later or not at all for coniferous trees. On the other hand, the nutrient, water and sunlight availability lead to a variability of vegetation activity even among the same species. Factors like the location and the surroundings of a species are therefore responsible for the variation in EOS rather than just biodiversity. Richardson et al. (2009) found in their study that the green-down takes much longer than the green-up and observed also a broader variation within deciduous forests among the EOS dates than SOS dates.

The variation of the phenology metrics at Laegern is about the same size for the near-surface and the remote-sensing analysis (15 and 19 days respectively). This is more than expected from previous studies in a similar ecosystem such as the one of Richardson et al. (2009). These findings suggest that the methods are suitable to measure PP and therefore to detect biodiversity and ecological processes on the level of single plants or plant communities. However, the range of the extracted dates differs between the two observation methods. The observation with remotely-sensed data revealed an earlier green-up and earlier SOS dates. The different 50-percent values can partly be explained with the smaller amplitude of GCC from the remotely-sensed data. Because the perception of greenness depends on the sensor and the atmosphere between sensor and

vegetation, differences in the amplitude of greenness occur. The 50-percent threshold is furthermore a mathematical rather than a biological characteristic. However, the satellite measurements also detected an earlier green-up. One reason might be the different viewing angles. As the satellite sensor points vertically to the ground, it also measures signals from the forest floor during the time the trees are leafless, whereas the phenocam ROIs contained almost no ground signals from the background of the examined tree. As grasses and small plants on the forest floor tend to start growing earlier than the leaves of the trees (due to the greater sunlight availability), satellite sensors could measure an overall earlier green-up than the phenocam at the deciduous forest test site. This assumption finds support by the analysis of Mizunuma et al. (2013) and D'Odorico et al. (2015). Both studies detected an earlier green-up with a downward looking camera, compared to the oblique looking phenocam and attributed this to the understory vegetation. D'Odorico et al. (2015) further mentioned, that this finding does not apply for satellite data at a coarse spatial resolution because a much larger area is integrated. The comparison of the phenocam metrics with the remotely-sensed datasets at the Laegern test site fits this theory. The four datasets consisting of high-resolution satellite data (Sentinel 2, Landsat 8, S2L8 and L8SR) detected an earlier and MODIS a later SOS than the phenocam.

In Kytalyk, the distinction between grass and shrubs was possible. Shrubs showed an earlier green-up and a lower maximum of greenness values compared to grass. The study of Sweet et al. (2015) supports the observation of an earlier green-up for shrubs. This information could successfully be transferred to the satellite data analysing PP as two groups are discernible in the data (Figure C.4). Being able to detect the phenology of functional groups by analysing pixels of high-resolution satellite data can be used as an indicator for shrub encroachment (Sweet et al., 2015, Myers-Smith and Hik, 2018) and consequently to analyse its ecological influence and its drivers (e.g. Myers-Smith et al., 2015). It has to be considered, however, that in Kytalyk NDVI and GCC data were compared and that in the phenocam data the distinction of the two vegetation types was no longer possible for the second site year (2016).

5.2 Data Stability

The ratio of the green colour in the reference panel at Laegern test site was stable over the seasons, the normalisation that was performed by calculating CC already eliminated the effects caused by different diurnal and seasonal illumination strengths. The lower values, caused by darkness, were removed when performing a maximum filtering (Figure 4.2, Section 4.2). It was therefore not necessary to use the reference panel.

Additionally, the reference panel does not account for the variable illumination of vegetation. The illumination of vegetation is not homogeneous, the values of the reference panel are therefore not suitable for correcting the variation in illumination within a ROI. The reference panel can however be used to detect images with major disturbances. Because the calculation of CC already normalises the data and the reference panel does not account for the heterogenous illumination of vegetation, it was not used for the analysis in this thesis.

The analysis of the influence of images with weather disturbances has shown, that normalising the data by calculating CC and using a maximum-filter afterwards, suffices to account for such influences. However, this does not account for satellite data: due to the smaller number of images, more than three consecutive measurements with cloud disturbances led to values that did not represent vegetation, whereas in the phenocam data even in longer rainy or foggy periods, vegetation was visible very regularly. Only heavy snow cover for several days or weeks would have an influence on the data.

5.3 Linking Plant Phenology and Land Surface Phenology

For answering the second research question, quantitative and ecological differences between PP and LSP were assessed. Extracted metrics from PP and LSP lay in a range of maximum 14 days for the deciduous forest and 18 days for the tundra test site (without outliers of unsuccessful analyses) and the metrics of the whole phenocam image always lay within that range (Table B-5).

So far, studies that compared satellite and phenocam observations, found that the derived phenological transition dates were not equivalent but did correlate (D'Odorico et al., 2015; Rodriguez-Galiano et al., 2015; Baumann et al., 2017; Liu et al., 2017). The

studies of Hufkens et al. (2012) and Klosterman et al. (2014) did not detect a correlation between the measurements of the two paradigms, mainly because of a too small site-year sample. Hufkens et al. (2012) argue, that the satellite measurements with a much lower temporal or spatial resolution cannot be expected to be as precise as the phenocam metrics. To analyse the correlation between the near-surface and remote sensing metrics however, many more years are necessary than the ones used in this study. The derived results of this study allow to qualitatively analyse the abovementioned viewing angle of the sensors, the FOV of the phenocam, the level of processing of the data and the quality of the used fits.

Camera angle

As described in section 5.1, the high-resolution satellite data detected an earlier SOS and the MODIS data a later SOS than the phenocam measurements for the deciduous forest. It is expected, that the nadir view of the satellite discovers understory vegetation with an earlier green-up (Mizunuma et al., 2013; D'Odorico et al., 2015), whereas the coarse resolution of MODIS integrates a much larger area which reduces this effect.

FOV of the phenocam

Comparing the PP (single pixels in the FOV of the camera) and the LSP measurements from Sentinel-2 data, shows that the metrics for the whole test site lay within the range of the PP metrics for both Laegern and Kytalyk test site. Therefore, it can be assumed that the FOV of the camera is representative of the whole test site and that thus, the measurements of the camera can be extrapolated to the larger area. At the Tibetan test site, however, the FOV of the phenocam is not perfectly representative of the whole test site as the SOS and EOS metrics of the whole test site are outside the range of the pixels in the FOV of the camera (Table C-6 and Figure C.5). But even if the vegetation in the FOV is representative of the whole test site, further analysis of single species with different surroundings or illumination conditions would be necessary to find out whether the measurements of one point show the same transition dates under slightly different conditions and are therefore suitable to be extrapolated. Analyses of ROIs containing the same species in the deciduous forest and the tundra have shown different phenology

metrics. Small variations of transition dates have thus to be expected even within a vegetation species.

If the FOV is representative of the larger area, phenocam data could also be used to validate satellite data. Due to the temporal resolution, it can be expected, that the uncertainty of the satellite data is much larger than the one of the phenocams. Still, the different viewing angle of the two sensors, with the satellite being more sensitive for understory vegetation in a deciduous forest, as well as the different characteristics of the sensors and the atmospheric influences lead to uncertainty when the two paradigms are compared. A phenocam with a nadir view and a comparison of metrics like the start of green-up or the peak of greenness would therefore be more appropriate to validate LSP measurements using phenocam data.

Level of data processing

The GCC values derived from the TOA products of Landsat 8 and Sentinel 2 were much lower than the ones from the SR data from MODIS and Landsat 8. Responsible for that was the different level of processing of the data. Even though this should not have affected the phenology metrics because they were extracted as relative and not absolute values, the analysis of some datasets led to inaccurate results (e.g. Landsat-8 and Sentinel-2 data in Kytalyk).

The amplitude of the GCC values derived from the phenocam lay between the TOA and SR datasets in Laegern and Haibei; in Kytalyk the amplitude was even higher than for the SR data. NDVI data did not show differences between TOA and SR data as the influence of the atmosphere at higher latitudes was strongest in the blue and green channels.

Quality of curve fits

LSP measurements at the tundra test site revealed a longer season and earlier green-up than measured in situ. The NDVI increased even earlier than GCC. On the one hand, this confirms the findings of Walther et al. (2016) that greenness lags behind photosynthesis, particularly at high latitudes. On the other hand, both indices increased at times when the ground was still covered by snow (snow lay until 1st June in 2016/DOY 153). The

main reason for this issue is the curve fit, that did not account for the short decrease of NDVI before the increase (Figure 5.1) and therefore showed an untimely green-up. Satellite-derived GCC values increased slightly during the last days of snowmelt due to changes in the colour of the snow. A possibility to account for these issues is to flag images with snow cover and just use data that shows vegetation. Moreover, the spline fit underestimates the amplitude of NDVI values, due to lower values that drag the curve down. This could be mitigated by iterative fitting while eliminating values that deviate more than a threshold from the expected (fitted) value.

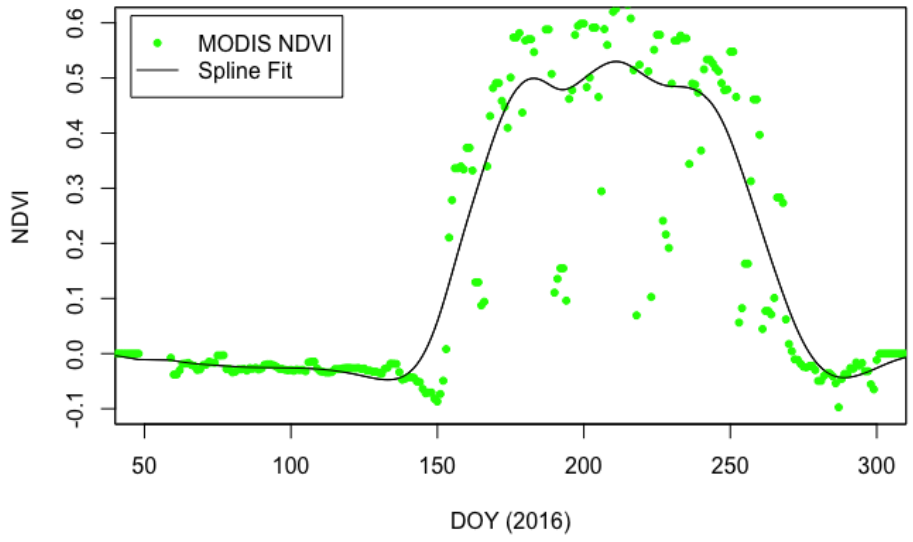

Figure 5.1: Spline fit and maximum-filtered MODIS NDVI data from Kytalyk test site 2016. After day of year (DOY) 140, the NDVI values decrease but the fitted curve already increases.

5.4 Comparison of GCC and NDVI

The analysis of the MODIS data showed, that NDVI derived phenology metrics led to a longer season than metrics of GCC data. Furthermore, the SOS and EOS dates only correlated in Kytalyk for the GCC and NDVI data. An earlier SOS in the NDVI data at the Laegern test site did not necessarily lead to an earlier SOS in the GCC data. The Sentinel-2 data and the merged dataset S2L8, however, showed a later SOS with NDVI data than with GCC data. The most probable reasons for this are the different widths and centre wavelengths of the satellite bands.

The findings of the MODIS time series analysis accord with the studies of Keenan et al. (2014) and Walther et al. (2016). The earlier onset and later end of vegetation activity

measured with NDVI data compared to the greenness derived metrics, coincide with the theory, that photosynthetic activity starts earlier than the increase of greenness, and that in autumn the greenness decreases earlier than the photosynthesis rate. As NDVI is supposed to be more sensitive to photosynthesis than GCC, the index detects earlier SOS and later EOS dates. Also, a visible inspection of the phenocam images from Kytalyk showed that the GCC decreased while vegetation turned red (end of August, DOY 230 to 240), whereas the NDVI decreased rather quickly three to four weeks later (EOS at DOY 259 and 261). The NDVI reached a value of 0 at about the same time the first snow fell (DOY 269). As described by Walther et al. (2016), the effect of a longer photosynthesis rate compared to greenness was stronger at high latitudes, and GCC and NDVI coincided better for the deciduous forest. Furthermore, the variation of phenology metrics derived from the sixteen Sentinel-2 pixels in the FOV of the phenocam was smaller for the NDVI data than for the GCC data. A qualitative reason for this difference might be, that the colour development between the species varies more than the photosynthetic activity.

The comparison of the two indices in combination with a visual inspection of the phenocam images and the ecological knowledge about the test sites greatly improves relating biological events, phenology measurements, greenness and plant activity.

5.5 Limitations

Several factors involved can limit the success of the analysis. From the data part, limitations can stem from the data availability and quality. Regarding the methods, the definition of ROIs, the filtering, fitting, index choice and extraction method can lead to errors or uncertainties.

Data availability of satellite imagery is limited; the availability of phenocam images every hour and of L8SR data in Kytalyk once every two weeks leads automatically to a different level of uncertainty. This issue however was well-known in advance (e.g. Hufkens et al., 2012). The simplest measures to improve the availability is merging products from different sensors. Concerning the data quality, cloud disturbance is the major issue for satellite data. Besides cloud cover, the second factor responsible for the data quality is the influence of the atmosphere upon the TOA products. At high latitudes like in Kytalyk,

the TOA data could not be used, a correction to surface-reflectance level would have been necessary first. The data quality and availability of phenocam images was stable and already analysed in Section 5.2. The only factor that was not analysed are systematic errors such as the viewing angle or the illumination. Because the camera is facing vegetation sideways, there is always some vegetation analysed, that is covered in shade. This effect is smaller with satellite data, as the satellites orbit the earth in a sun-synchronous mode. With the phenocam pointing north, this effect is minimised.

Further sources of error can occur during the processing of the data. Firstly, the definition of ROIs was implemented arbitrarily. The selection of trees of the deciduous forest as well as the size of the ROI for the LSP analysis could have been chosen differently and therefore probably could have affected the results. The filtering method was without a doubt suitable for the phenocam images with their availability of one image per hour. Choosing the window size for the satellite data was more delicate. With a window size of three measurements, three consecutive overcast days led to data that did not represent vegetation. A larger window size on the other hand would have taken the maximum value of a time span of three weeks and more for Sentinel-2 and Landsat-8 data which would have led to a much greater uncertainty in the received data. For datasets with scarcer image availability, a cloud filter would be more valuable than a maximum-filter. A successful filtering of the data facilitates the fitting of a curve. The use of predefined fitting algorithms (Spline, Beck and Klosterman fits, Filippa et al., 2016) made it necessary to use different curve fitting methods for different datasets (Section 3.4). As a consequence, the different datasets were more difficult to compare, because of slight differences in the shape of the curves. The spline fit was closer to the actual data and therefore more sensitive to outliers or cloud disturbances whereas the Beck and the Klosterman fits were more robust but therefore capturing small variations less precisely. For instance, the curve fitted into the MODIS data is below the maximum values because of lower values, caused by cloud disturbances, dragging the curve down (Figure 5.1). For the Sentinel-2 data, the Klosterman fit would have had a smaller RMSE, but it did not account for the maximum values, therefore the Beck fit was chosen.

The choice of the vegetation index and the method to determine the SOS and EOS has mainly influenced the phenology metrics. The 50-percent value as well as the maximum increase of the curve are generally not related to a biological process (D'Odorico et al., 2015). The maximum change of curvature of a greenness index like GCC could be related to the start of vegetation green-up. Furthermore, as discussed in Section 3.6, photosynthetic activity is difficult to relate to greenness. But although the chosen indices or extraction methods are not directly relatable to biological events, they allowed a comparison between the different observation methods and datasets.

Quantify uncertainty

Besides the detection of sources for uncertainty, the quantification of the uncertainty is of great interest. Considering the uncertainties that are created by the abundance of data, the frequency of clouds, the different fitting methods and the few site years, the margin of error can easily be larger than the differences between the compared data. Besides the RMSE for the fitted curves, the number of data points available during the green-up period could work as an accuracy metric under the condition that clouds are accurately filtered. The example of the Laegern test site shows that the uncertainty of the Landsat SR curve is accordingly much higher than for MODIS and the phenocam data. The green-up period of the L8SR dataset contained 4 measurements whereas MODIS and the phenocam provide 50 measurements each for the same time-span. The MODIS data, however, contained an unknown number of measurements affected by clouds.

5.6 Outlook

The presented analysis has shown a method of applying phenocam and high-resolution satellite data in order to determine biodiversity and link PP and LSP. The findings can clearly be enhanced by a more sophisticated preparation of satellite data (cloud and snow filtering, processing to SR) and an analysis of more site years. With the launch of the second Sentinel-2 satellite, the availability of high-resolution satellite imagery has increased relevantly and applying the presented method to a vast number of site years allows detecting correlations between different datasets and between phenology measurements at different scales.

Analysing more site years and more different biomes will lead to a better understanding between the relations of small- and large-scale phenology patterns and allow relating biological processes to phenological metrics as well as scaling between species, community and ecosystem.

6 Conclusion

In line with the two blocks of research questions, the findings of the thesis are briefly summarised.

Measuring plant phenology (PP) with phenocam and high-resolution satellite data

The analysis of PP has revealed that biodiversity can be assessed, and the phenological characteristics of single species analysed, with both phenocam and high-resolution satellite imagery. The presented method therefore enables an analysis of whether changes in land surface phenology (LSP) are climate driven, like a shift in the growing season length of a plant, or due to changes in biodiversity and the appearance of ecological niches. For a successful comparison of near-surface and remotely-sensed data, a representative field of view of the camera is crucial and the different viewing angle and atmospheric influences are important to consider when explaining shifts in the results.

Normalising and filtering the phenocam data suffices for successful modelling of vegetation activity, for satellite imagery a cloud and snow filter would be necessary for a precise vegetation analysis.

Correspondence and relation between PP and LSP

The results of the PP analysis show, that the method used is suitable to detect ecological processes on species level. The high spatial resolution of Sentinel 2 enables new options to measure PP with a world-wide coverage and to compare and upscale it to LSP. Phenocams, in return, allow relating biological processes to the PP measurements either by inspecting images or with the support of ecological knowledge about the examined test sites. The combination of the two measurement techniques therefore facilitates the understanding of influences of environmental processes at community level (e.g., shrub encroachment, growth of understory vegetation, shifts in ecological niches, shifts in phenology), on an ecosystem, or even on a global level.

Even though phenology metrics of the different sensors lay within two weeks per test site (without obvious outliers), comparing satellite-derived LSP with PP measurements quantitatively proved to be more complicated. Differences between the different datasets

were often larger than between the phenocam and a satellite sensor itself. Qualitative differences and sources of uncertainty could be evaluated, but for a quantitative analysis like the correlation between the different measurements, many more site years are necessary.

NDVI tends to be sensitive for vegetation activity earlier during green-up and longer during senescence than green chromatic coordinates (GCC). The findings corroborate the theory on greenness and photosynthetic activity of the two indices from Keenan et al. (2014) and D'Odorico et al. (2015). NDVI is more sensitive to photosynthetic activity than GCC and greenness usually lags behind photosynthesis during green-up and lasts longer during senescence. The relation between greenness and photosynthesis rate gives important insights on carbon fluxes and on the relation between phenology measurements and biological processes. However, exceptions were detected and the findings of the relation between the two indices are always dependent on the method, test site and satellite sensor (Sections 3.6 and 5.4).

Acknowledgements

First and foremost, I would like to thank my supervisor Dr. Rogier de Jong for his dedicated support over the whole year and his willingness to advise me wherever he could and whenever possible. Furthermore, I would like to express my gratitude to Claudia Röösli for her valued inputs on satellite data, Gillian Milani for providing me with PyCharm code and to Franziska Moergeli and Steven Hawkes for their appreciated suggestions and inputs concerning the whole thesis. Last but not least I want to thank my parents for their everlasting support during my whole studies.

Literature

Ahrends, H.E., Bräugger, R., Stöckli, R., Schenk, J., Michna, P., Jeanneret, F., Wanner, H., Eugster, W., 2008. Quantitative phenological observations of a mixed beech forest in northern Switzerland with digital photography. J. Geophys. Res. Biogeosciences 113. https://doi.org/10.1029/2007JG000650

Baldocchi, D.D., Black, T.A., Curtis, P.S., Falge, E., Fuentes, J.D., Granier, A., Gu, L., Knohl, A., Pilegaard, K., Schmid, H.P., Valentini, R., Wilson, K., Wofsy, S., Xu, L., Yamamoto, S., 2005. Predicting the onset of net carbon uptake by deciduous forests with soil temperature and climate data: A synthesis of FLUXNET data. Int. J. Biometeorol. 49, 377–387. https://doi.org/10.1007/s00484-005-0256-4

Baumann, M., Ozdogan, M., Richardson, A.D., Radeloff, V.C., 2017. Phenology from Landsat when data is scarce: Using MODIS and Dynamic Time-Warping to combine multi-year Landsat imagery to derive annual phenology curves. Int. J. Appl. Earth Obs. Geoinf. 54, 72–83. https://doi.org/10.1016/j.jag.2016.09.005

Beck, P.S.A., Atzberger, C., Høgda, K.A., Johansen, B., Skidmore, A.K., 2006. Improved monitoring of vegetation dynamics at very high latitudes: A new method using MODIS NDVI. Remote Sens. Environ. 100, 321–334. https://doi.org/10.1016/j.rse.2005.10.021

Brown, T.B., Hultine, K.R., Steltzer, H., Denny, E.G., Denslow, M.W., Granados, J., Henderson, S., Moore, D., Nagai, S., Sanclements, M., Sánchez-azofeifa, A., Sonnentag, O., Tazik, D., Richardson, A.D., 2016. Using phenocams to monitor our changing Earth: toward a global phenocam network In a nutshell: Front. Ecol. Environ. 14, 84–93. https://doi.org/10.1002/fee.1222

Cleland, E.E., Chuine, I., Menzel, A., Mooney, H.A., Schwartz, M.D., 2007. Shifting plant phenology in response to global change. Trends Ecol. Evol. 22, 357–365. https://doi.org/10.1016/j.tree.2007.04.003

D'Odorico, P., Gonsamo, A., Gough, C.M., Bohrer, G., Morison, J., Wilkinson, M., Hanson, P.J., Gianelle, D., Fuentes, J.D., Buchmann, N., 2015. The match and mismatch between photosynthesis and land surface phenology of deciduous forests. Agric. For. Meteorol. 214–215, 25–38. https://doi.org/10.1016/j.agrformet.2015.07.005

Elmore, A.J., Guinn, S.M., Minsley, B.J., Richardson, A.D., 2012. Landscape controls on the timing of spring, autumn, and growing season length in mid-Atlantic forests. Glob. Chang. Biol. 18, 656–674. https://doi.org/10.1111/j.1365-2486.2011.02521.x

ESA Earth Online: Mission Details, 2018. (https://earth.esa.int/web/guest/missions/esa-operational-eo-missions/sentinel-2[22.3.2018]).

Filippa, G., Cremonese, E., Migliavacca, M., Galvagno, M., Forkel, M., Wingate, L., Tomelleri, E., Morra, U., Richardson, A.D., 2016. Agricultural and Forest Meteorology Phenopix: A R package for image-based vegetation phenology. Agric. For. Meteorol. 220, 141–150. https://doi.org/10.1016/j.agrformet.2016.01.006

Fisher, J.I., Mustard, J.F., Vadeboncoeur, M.A., 2006. Green leaf phenology at Landsat resolution: Scaling from the field to the satellite. Remote Sens. Environ. 100, 265–279. https://doi.org/10.1016/j.rse.2005.10.022

Fitzjarrald, D. R., Acevedo, O. C., & Moore, K. E., 2001. Climatic consequences of leaf presence in the eastern United States. *Journal of Climate*, *14*(4), 598–614. https://doi.org/10.1175/1520-0442(2001)014<0598:CCOLPI>2.0.CO;2

Flickr, 2011. TimeScience VRG phenocam install. (https://www.flickr.com/photos/timescience/6261036769 [20.10.2017]).

Garonna, I., De Jong, R., Schaepman, M.E., 2016. Variability and evolution of global land surface phenology over the past three decades (1982 – 2012). Glob. Chang. Biol. 22, 1456–1468. https://doi.org/10.1111/gcb.13168

Gillespie, A.R., Kahle, A.B., Walker, R.E., 1987. Color enhancement of highly correlated images. II. Channel ratio and "chromaticity" transformation techniques. Remote Sens. Enrivon. 22, 343-365.

Gorelick, N., Hancher, M., Dixon, M., Ilyushchenko, S., Thau, D., & Moore, R., 2017. Google Earth Engine: Planetary-scale geospatial analysis for everyone. Remote Sensing of Environment.

Goulden, M. L., Munger, J. W., Fan, S. M., Daube, B. C., & Wofsy, S. C., 1996. Exchange of carbon dioxide by a deciduous forest: Response to interannual climate variability. *Science*, *271*(5255), 1576–1578. https://doi.org/10.1126/science.271.5255.1576

Gu, L., Post, W.M., Baldocchi, D.D., Black, T.A., Suyker, A.E., Verma, S.B., Vesala, T., Wofsy, S.C., 2009. Characterizing the seasonal dynamics of plant community photosynthesis across a range of vegetation types, in: Phenology of Ecosystem Processes: Applications in Global Change Research. pp. 35–58. https://doi.org/10.1007/978-1-4419-0026-5_2

Hufkens, K., Friedl, M., Sonnentag, O., Braswell, B.H., Milliman, T., Richardson, A.D., 2012. Linking near-surface and satellite remote sensing measurements of deciduous broadleaf forest phenology. Remote Sens. Environ. 117, 307–321. https://doi.org/10.1016/j.rse.2011.10.006

Inoue, T., Nagai, S., Kobayashi, H., Koizumi, H., 2015. Utilization of ground-based digital photography for the evaluation of seasonal changes in the aboveground green biomass and foliage phenology in a grassland ecosystem. Ecol. Inform. 25, 1–9. https://doi.org/10.1016/j.ecoinf.2014.09.013

JetBrains, 2017: PyCharm. (https://www.jetbrains.com/pycharm/[10.11.2017]).

Keenan, T.F., Darby, B., Felts, E., Sonnentag, O., Friedl, M.A., Hufkens, K., O'Keefe, J., Klosterman, S., Munger, J.W., Toomey, M., Richardson, A.D., 2014. Tracking forest phenology and seasonal physiology using digital repeat photography: A critical assessment. Ecol. Appl. 24. https://doi.org/10.1890/13-0652.1

Klosterman, S.T., Hufkens, K., Gray, J.M., Melaas, E., Sonnentag, O., Lavine, I., Mitchell, L., Norman, R., 2014. Evaluating remote sensing of deciduous forest phenology at multiple spatial scales using PhenoCam imagery. Biogeosciences 11, 4305–4320. https://doi.org/10.5194/bg-11-4305-2014

Liang, L., Schwartz, M.D., Fei, S., 2011. Validating satellite phenology through intensive ground observation and landscape scaling in a mixed seasonal forest. Remote Sens. Environ. 115, 143–157. https://doi.org/10.1016/j.rse.2010.08.013

Lieth, H.H., 1976. Contributions to phenology seasonality research. Int. J. Biometeorol. 20, 197–199. https://doi.org/10.1007/BF01553661

Liu, Y., Hill, M.J., Zhang, X., Wang, Z., Richardson, A.D., Hufkens, K., Filippa, G., Baldocchi, D.D., Ma, S., Verfaillie, J., Schaaf, C.B., 2017. Using data from Landsat, MODIS, VIIRS and PhenoCams to monitor the phenology of California oak/grass savanna and open grassland across spatial scales. Agric. For. Meteorol. 237–238, 311–325. https://doi.org/10.1016/j.agrformet.2017.02.026

Menzel, A., 2002. Phenology: Its importance to the global change community: An editorial comment. *Climatic Change*. https://doi.org/10.1023/A:1016125215496

Menzel, A., Sparks, T. H., Estrella, N., Koch, E., Aaasa, A., Ahas, R., … Zust, A., 2006. European phenological response to climate change matches the warming pattern. *Global Change Biology*, *12*(10), 1969–1976. https://doi.org/10.1111/j.1365-2486.2006.01193.x

Mizunuma, T., Wilkinson, M., L. Eaton, E., Mencuccini, M., I. L. Morison, J., Grace, J., 2013. The relationship between carbon dioxide uptake and canopy colour from two camera systems in a deciduous forest in southern England. Funct. Ecol. 27, 196–207. https://doi.org/10.1111/1365-2435.12026

MODIS, 2017: MODIS design. (https://modis.gsfc.nasa.gov/about/design.php[22.2.2018]).

Myers-Smith, I. H., Elmendorf, S. C., Beck, P. S. A., Wilmking, M., Hallinger, M., Blok, D., … Vellend, M., 2015. Climate sensitivity of shrub growth across the tundra biome. *Nature Climate Change*, *5*(9), 887–891. https://doi.org/10.1038/nclimate2697

Myers-Smith, I. H., & Hik, D. S., 2018. Climate warming as a driver of tundra shrubline advance. *Journal of Ecology*, *106*(2), 547–560. https://doi.org/10.1111/1365-2745.12817

Nemani, R. R., Keeling, C. D., Hashimoto, H., Jolly, W. M., Piper, S. C., Tucker, C. J., … Running, S. W., 2003. Climate-driven increases in global terrestrial net primary production from 1982 to 1999. *Science*, *300*(5625), 1560–1563. https://doi.org/10.1126/science.1082750

Nijland, W., Bolton, D.K., Coops, N.C., Stenhouse, G., 2016. Imaging phenology; scaling from camera plots to landscapes. Remote Sens. Environ. 177, 13–20. https://doi.org/10.1016/j.rse.2016.02.018

Nijland, W., Jong, R. De, Jong, S.M. De, Wulder, M.A., Bater, C.W., Coops, N.C., 2014. Agricultural and Forest Meteorology Monitoring plant condition and phenology using infrared sensitive consumer grade digital cameras. Agric. For. Meteorol. 184, 98–106. https://doi.org/10.1016/j.agrformet.2013.09.007

NOAA Satellite Information System, 2017: Advanced Very High Resolution Radiometer – AVHRR. (http://noaasis.noaa.gov/NOAASIS/ml/avhrr.html[22.1.2018]).

Parmesan, C., 2007. Influences of species, latitudes and methodologies on estimates of phenological response to global warming. Glob. Chang. Biol. 13, 1860–1872. https://doi.org/10.1111/j.1365-2486.2007.01404.x

Penuelas, J., Rutishauser, T., Filella, I., 2009. Phenology Feedbacks on Climate Change. Science 324, 887–888. https://doi.org/10.1126/science.1173004

Pereira, H.M., Ferrier, S., Walters, M., Geller, G.N., Jongman, R.H.G., Scholes, R.J., Bruford, M.W., Brummitt, N., Butchart, S.H.M., Cardoso, A.C., Coops, N.C., Dulloo, E., Faith, D.P., Freyhof, J., Gregory, R.D., Heip, C., Höft, R., Hurtt, G., Jetz, W., Karp, D.S., McGeoch, M.A., Obura, D., Onoda, Y., Pettorelli, N., Reyers, B., Sayre, R., Scharlemann, J.P.W., Stuart, S.N., Turak, E., Walpole, M., Wegmann, M., 2013. Essential Biodiversity Variables. Science 339, 277–278. https://doi.org/10.1126/science.1229931

R Development Core Team, 2008. R: A language and environment for statistical computing. R Foundation for Statistical Computing, Vienna, Austria. ISBN 3-900051-07-0, URL http://www.R-project.org.

Richardson, A.D., Anderson, R.S., Arain, M.A., Barr, A.G., Bohrer, G., Chen, G., Chen, J.M., Ciais, P., Davis, K.J., Desai, A.R., Dietze, M.C., Dragoni, D., Garrity, S.R., Gough, C.M., Grant, R., Hollinger, D.Y., Margolis, H.A., Mccaughey, H., Migliavacca, M., Monson, R.K., Munger, J.W., Poulter, B., Raczka, B.M., Ricciuto, D.M., Sahoo, A.K., Schaefer, K., Tian, H., Vargas, R., Verbeeck, H., Xiao, J., Xue, Y., 2012. Terrestrial biosphere models need better representation of vegetation phenology: Results from the North American Carbon Program Site Synthesis. Glob. Chang. Biol. 18, 566–584. https://doi.org/10.1111/j.1365-2486.2011.02562.x

Richardson, A. D., Bailey, A. S., Denny, E. G., Martin, C. W., & O'Keefe, J., 2006. Phenology of a northern hardwood forest canopy. *Global Change Biology*, *12*(7), 1174–1188. https://doi.org/10.1111/j.1365-2486.2006.01164.x

Richardson, A.D., Braswell, B.H., Hollinger, D.Y., Jenkins, J.P., Ollinger, S. V., 2009. Near-surface remote sensing of spatial and temporal variation in canopy phenology. Ecol. Appl. 19, 1417–1428. https://doi.org/10.1890/08-2022.1

Richardson, A.D., Jenkins, J.P., Braswell, B.H., Hollinger, D.Y., Ollinger, S. V., Smith, M.L., 2007. Use of digital webcam images to track spring green-up in a deciduous broadleaf forest. Oecologia 152, 323–334. https://doi.org/10.1007/s00442-006-0657-z

Richardson, A. D., Klosterman, S., & Toomey, M., 2013. Near-surface sensor-derived phenology. In *Phenology: An Integrative Environmental Science* (Vol. 9789400769250, pp. 413–430). https://doi.org/10.1007/978-94-007-6925-0_22

Rodriguez-Galiano, V.F., Dash, J., Atkinson, P.M., 2015. Intercomparison of satellite sensor land surface phenology and ground phenology in Europe. Geophys. Res. Lett. 42, 2253–2260. https://doi.org/10.1002/2015GL063586

Schwartz, M.D., Hanes, J.M., 2010. Intercomparing multiple measures of the onset of spring in eastern North America. Int. J. Climatol. 30, 1614–1626. https://doi.org/10.1002/joc.2008

Skidmore, A.K., Pettorelli, N., Coops, N.C., Geller, G.N., Hansen, M., Lucas, R., Mücher, C.A., O'Connor, B., Paganini, M., Pereira, H.M., Schaepman, M.E., Turner, W., Wang, T., Wegmann, M., 2015. Environmental science: Agree on biodiversity metrics to track from space. Nature 523, 403–405. https://doi.org/10.1038/523403a

Sonnentag, O., Hufkens, K., Teshera-sterne, C., Young, A.M., Friedl, M., Braswell, B.H., Milliman, T., Keefe, J.O., Richardson, A.D., 2012. Agricultural and Forest Meteorology Digital repeat photography for phenological research in forest ecosystems. Agric. For. Meteorol. 152, 159–177. https://doi.org/10.1016/j.agrformet.2011.09.009

Sparks, T.H., Menzel, A., 2002. Observed changes in seasons: An overview. Int. J. Climatol. 22, 1715–1725. https://doi.org/10.1002/joc.821

Sweet, S. K., Griffin, K. L., Steltzer, H., Gough, L., & Boelman, N. T., 2015. Greater deciduous shrub abundance extends tundra peak season and increases modeled net CO_2 uptake. *Global Change Biology*, *21*(6), 2394–2409. https://doi.org/10.1111/gcb.12852

Tang, Q., Oki, T., 2007. Daily NDVI relationship to cloud cover. J. Appl. Meteorol. Climatol. 46, 377–387. https://doi.org/10.1175/JAM2468.1

Tucker, C.J., 1979. Red and photographic infrared linear combinations for monitoring vegetation. Remote Sens. Environ. 8, 127–150. https://doi.org/10.1016/0034-4257(79)90013-0

URPP Global Change and Biodiversity, 2017: Test Sites. (http://www.gcb.uzh.ch/en/Research/TestSites.html[22.2.2018]).

URPP Global Change and Biodiversity, 2016a: Borneo. (http://www.gcb.uzh.ch/en/Research/TestSites/Malaysian.html[9.1.2018]).

URPP Global Change and Biodiversity, 2016b: Laegern. (http://www.gcb.uzh.ch/en/Research/TestSites/Laegeren.html[22.2.2018]).

URPP Global Change and Biodiversity, 2016c: Siberia. (http://www.gcb.uzh.ch/en/Research/TestSites/Siberia.html[22.2.2018]).

URPP Global Change and Biodiversity, 2016d: Aldabra. (http://www.gcb.uzh.ch/en/Research/TestSites/Aldbara.html[22.2.2018]).

Walther, S., Voigt, M., Thum, T., Gonsamo, A., Zhang, Y., Köhler, P., … Guanter, L., 2016. Satellite chlorophyll fluorescence measurements reveal large-scale decoupling of photosynthesis and greenness dynamics in boreal evergreen forests. *Global Change Biology*, *22*(9), 2979–2996. https://doi.org/10.1111/gcb.13200

White, M. A., & Nemani, R. R., 2006. Real-time monitoring and short-term forecasting of land surface phenology. *Remote Sensing of Environment*, *104*(1), 43–49. https://doi.org/10.1016/j.rse.2006.04.014

Woebbecke, D. M. Meyer, G.E. Von Bargen, K. & Mortensen, D. A., 1995. Color Indices for Weed Identification Under Various Soil, Residue, and Lighting Conditions. *Transactions of the ASAE*, *38*(1), 259–269. https://doi.org/10.13031/2013.27838

Zhang, X., Friedl, M. A., Schaaf, C. B., Strahler, A. H., Hodges, J. C. F., Gao, F., … Huete, A., 2003. Monitoring vegetation phenology using MODIS. *Remote Sensing of Environment*, *84*(3), 471–475. https://doi.org/10.1016/S0034-4257(02)00135-9

Appendix

A: Data

Table A-1: Tree species and abundances at Laegern test site (courtesy Carla Guillen Escriba).

Vegetation type	Family	Genus	Species	Total number individuals (% of total individuals)
D	Fagaceae	Fagus	sylvatica	518 (39.6)
D	Oleaceae	Fraxinus	excelsior	252 (19.3)
D	Sapindaceae	Acer	pseudoplatanus	168 (12.9)
C	Pinaceae	Abies	alba	108 (8.3)
D	Malvaceae	Tilia	platyphyllos	105 (8.0)
C	Pinaceae	Picea	abies	51 (3.9)
D	Ulmaceae	Ulmus	glabra	43 (3.3)
D	Sapindaceae	Acer	platanoides	40 (3.0)
D	Fagaceae	Quercus	petraea	9 (0.7)
D	Betulaceae	Carpinus	betulus	8 (0.6)
D	Sapindaceae	Acer	campestre	3 (0.2)
C	Pinaceae	Pinus	sylvestris	1 (0.1)
D	Rosaceae	Sorbus	aria	1 (0.1)
	Total families: 8	Total genus: 11	Total species: 13	Total individuals: 1307

D: deciduous. C: coniferous.

Table A-2: Spatial and temporal resolution of satellite data used (GEE, 2018).

	MODIS	**Landsat 8**	**Sentinel 2A**
Spatial resolution	500m	30m	10m
Temporal resolution (at the equator)	daily	16 days	10 days

Table A-3: Satellite images per year at the analysed test sites (GEE, 2018). In Kytalyk, Landsat 8 surface reflectance (L8 SR) has a smaller availability than the top of atmosphere images.

	MODIS	**Landsat 8**	**Sentinel 2**
Laegern 2016	355	37	67
Kytalyk 2015	364	45 (26 for L8 SR)	13
Kytalyk 2016	355	45 (22 for L8 SR)	80
Haibei 2015	364	44	3
Haibei 2016	355	44	72

Table A-4: Curve fitting methods for GCC and NDVI for the different satellite datasets. Abbreviations: top of atmosphere (TOA), merged Sentinel 2 and Landsat 8 dataset (S2L8), surface reflectance (SR).

Fitting method	**MODIS**	**Landsat 8 TOA**	**Sentinel 2**	**S2L8**	**Landsat 8 SR**
GCC	Spline	Beck	Beck	Klosterman	Klosterman (Laegern & Kytalyk), Beck (Haibei)
NDVI	Spline	Klosterman	Beck	Klosterman (Laegern & Haibei), Beck (Kytalyk)	Klosterman (Laegern & Kytalyk), Beck (Haibei)

B: Phenology Metrics

Table B-5: Phenology metrics showing start of season (SOS) and end of season (EOS) for the three test sites Laegern, Kytalyk and Haibei. Up to sixteen regions of interest (ROI) of phenocam data and MODIS, Sentinel-2, and Landsat-8 datasets were analysed. The metrics are depicted as day of year (DOY).

		Laegern 2016		Kytalyk 2015		Kytalyk 2016		Haibei 2015		Haibei 2016	
		SOS	**EOS**	**SOS**	**EOS**	**SOS**	**EOS**	**SOS**	**EOS**	**SOS**	**EOS**
Phenocam GCC	**ROI 1**	113	278	177	234	170	235		247	146	
	ROI 2	119	302	175	231	172	233				
	ROI 4	124	289	172	232	171	235				
	ROI 5	113	251	179	234	169	233				
	ROI 6	120	284	178	233						
	ROI 7	111	275								
	ROI 8	124	298								
	ROI 9	117	298								
	ROI 10	117	307								
	ROI 11	110	271								
	ROI 12	114	296								
	ROI 13	125	278								
	ROI 14	115	270								
	ROI 15	116	280								
	ROI 16	118	291								
	Whole Phenocam Image	113	278	178	233	171	235	no data	247	149	304
Satellite GCC	**Landsat 8**	106	239	142	255	102	293	154	287	155	273
	Sentinel 2	108	280			180	232			169	256
	MODIS	119	278	166	241	165	240	171	250	169	233
	Sentinel 2 & Landsat 8 (S2L8)	107	278			162	240			160	260
	Landsat 8 Surface Reflectance (L8SR)	107	318			165	245			155	276
Satellite NDVI	**Landsat 8**	101	279	148	264	155	274	176	297	167	292
	Sentinel 2	120	299			159	259			161	289
	MODIS	100	277	163	262	161	261	152	278	151	283
	S2L8	115	287			156	259			146	278
	L8SR	92	323			146	260			154	294

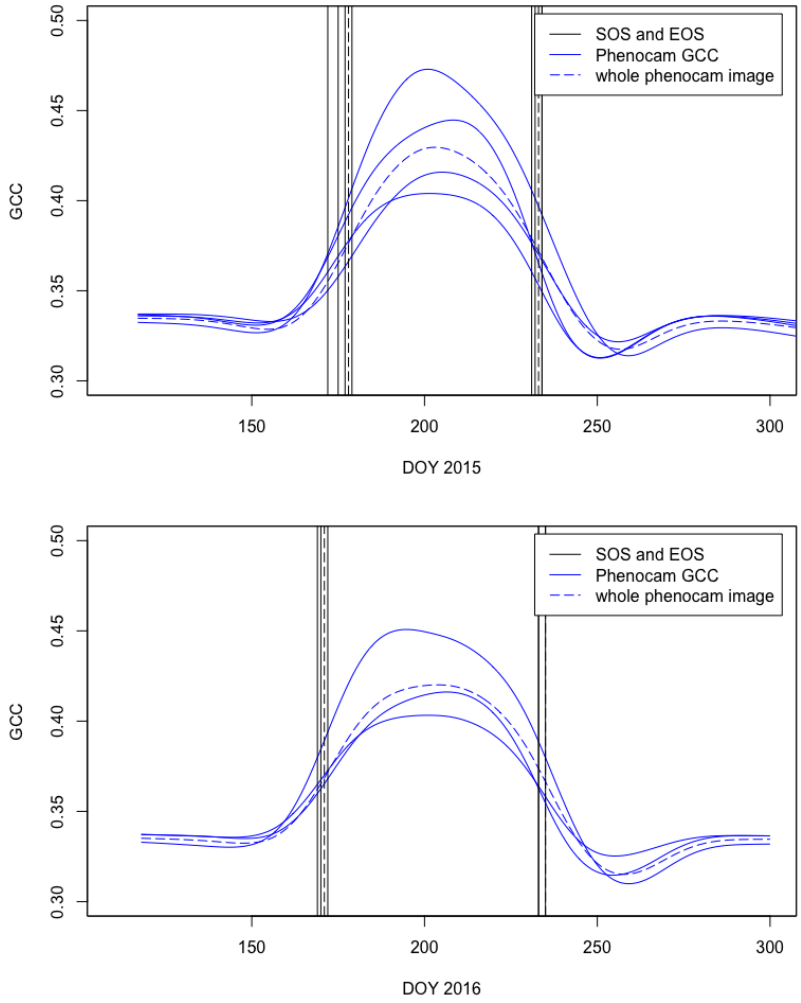

Figure B.1: Phenology curves of regions of interest (ROI) in the phenocam images at Kytalyk test site 2015 (top) and 2016 (bottom) with respective start of season (SOS) and end of season (EOS) as vertical lines. The dashed line represents the data from the ROI containing the whole phenocam image.

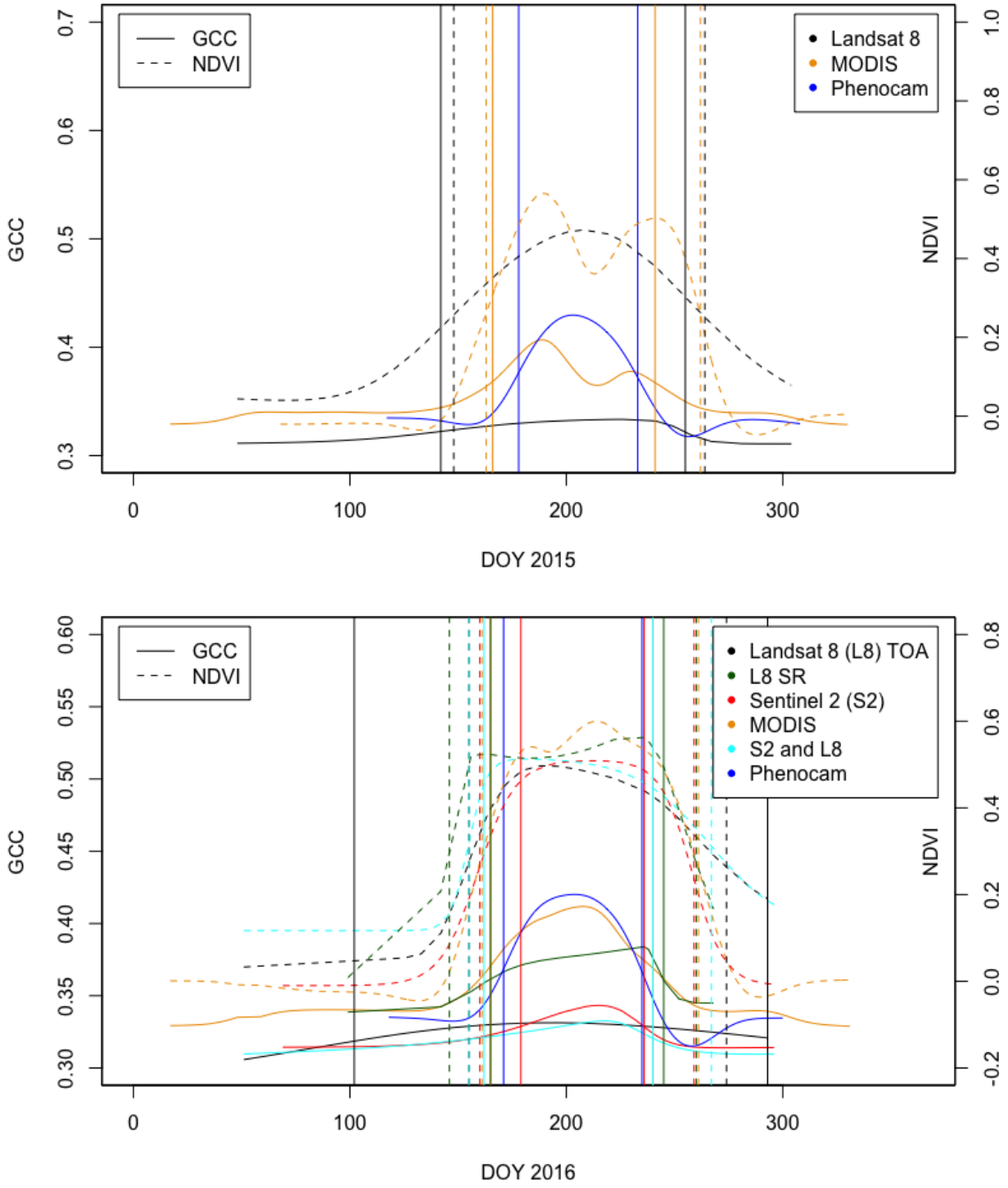

Figure B.2: Phenology curves from the satellite and phenocam datasets for Kytalyk 2015 and 2016 (top and bottom respectively). Both Landsat top of atmosphere (TOA) and surface reflectance (SR) data was used. The Sentinel-2 data also represents TOA-values. MODIS data is processed to model SR. The dashed lines stand for the NDVI data, the solid line for the GCC data. The vertical lines represent the start of season and end of season calculated with the 50-percent value.

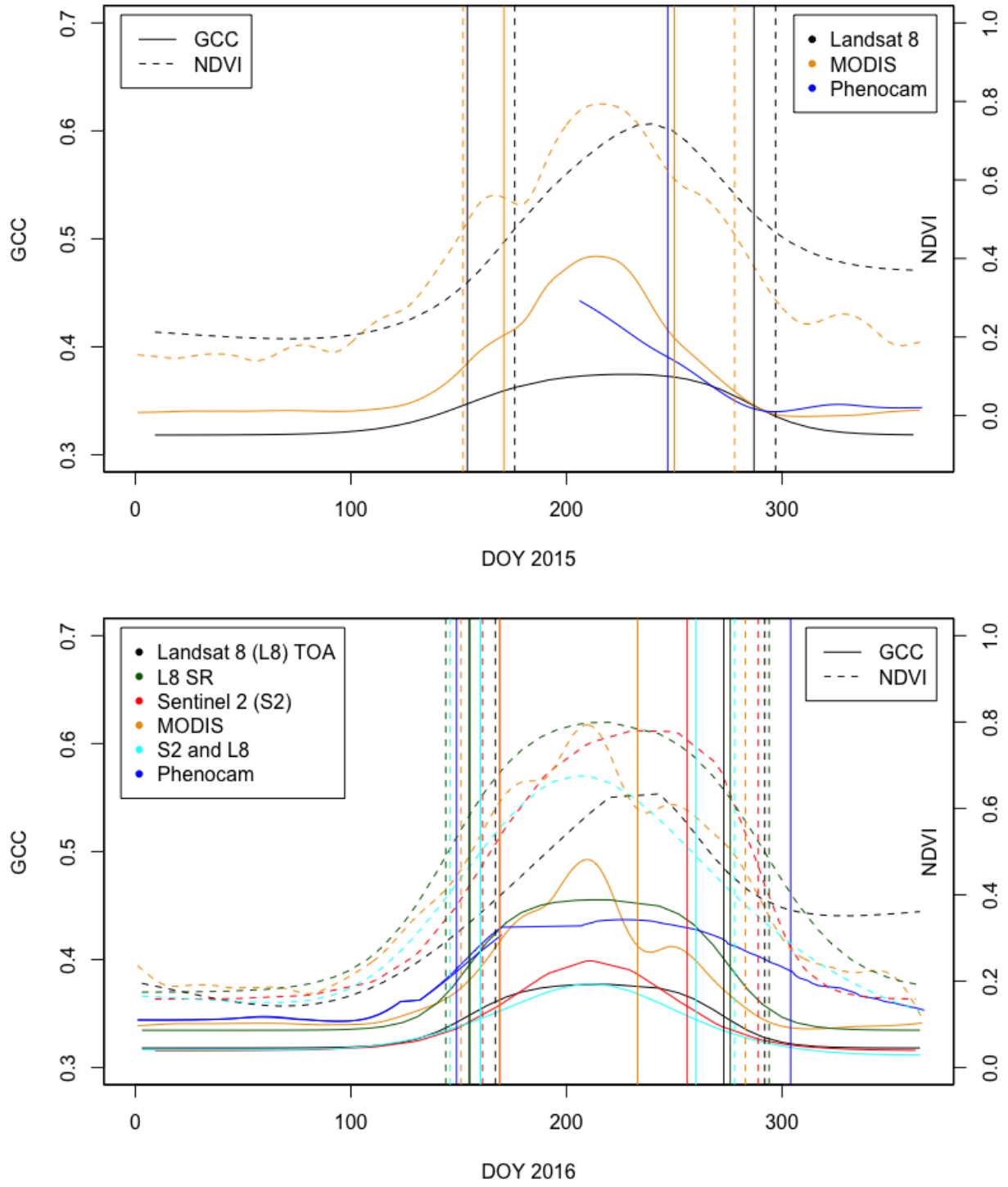

Figure B.3: Phenology curves from the satellite and phenocam datasets for Haibei 2015 and 2016 (top and bottom respectively). Both Landsat top of atmosphere (TOA) and surface reflectance (SR) data was used. The Sentinel-2 data also represents TOA-values. MODIS data is processed to model SR. The dashed lines stand for the NDVI data, the solid line for the GCC data. The vertical lines represent the start of season and end of season calculated with the 50-percent value. For the phenocam curve in Haibei 2016, the data from the second half of 2015 was taken as data for the second half of 2016.

C: Pixel-Wise Sentinel-2 Analysis

Table C-6: Phenology metrics of the analysis of sixteen Sentinel-2 pixels in the field of view of the phenocam at Laegern, Kytalyk and Haibei test site. Metrics are indicated as day of year. Minimal (Min) and maximal (Max) value, the mean of all measurements, the range between min and max and the standard deviation (Stdev) are indicated at the bottom of the table.

	Laegern				**Kytalyk**				**Haibei**			
	SOS		**EOS**		**SOS**		**EOS**		**SOS**		**EOS**	
ROI	**GCC**	**NDVI**	**GCC**	**NDVI**	**GCC**	**NDVI**	**GCC**	**NDVI**	**GCC**	**NDVI**	**GCC**	**NDVI**
1	93	111	282	309	132	160	260	260	165	153	262	286
2	102	109	264	312	154	169	256	258	161	152	265	290
3	94	114	284	294	124	168	266	259	162	152	266	286
4	108	122	286	295	166	173	246	258	167	153	262	286
5	96	114	283	290	130	161	262	259	164	154	262	287
6	94	111	279	295	159	171	255	257	164	153	265	291
7	97	108	282	297	137	162	265	260	160	153	266	290
8	109	111	281	298	131	158	266	261	163	153	262	287
9	100	112	264	291	129	165	263	258	164	156	264	287
10	97	108	283	297	150	168	258	257	164	153	260	287
11	105	109	256	289	150	171	260	258	163	153	262	288
12	102	116	258	285	124	160	267	260	164	154	262	288
13	110	115	274	299	131	161	265	260	NA	154	269	291
14	91	120	298	309	124	169	264	258	164	154	265	287
15	104	125	276	296	133	170	259	259	165	154	264	288
16	97	127	279	313	148	168	256	259	170	155	260	287
Whole test site	108	120	280	299	180	159	232	259	169	161	256	289
Min	91	108	256	285	124	158	246	257	160	152	260	286
Max	110	127	298	313	166	173	267	261	170	156	269	291
Mean	99.94	114.50	276.81	298.06	138.88	165.88	260.50	258.81	164	153.50	263.50	287.88
Range	19	19	42	28	42	15	21	4	10	4	9	5
Stdev	5.99	6.02	11.15	8.43	13.54	4.81	5.50	1.17	2.36	1.03	2.42	1.71
R^2	-0.0648		0.0856		0.0775		0.3564		-0.071		0.3304	

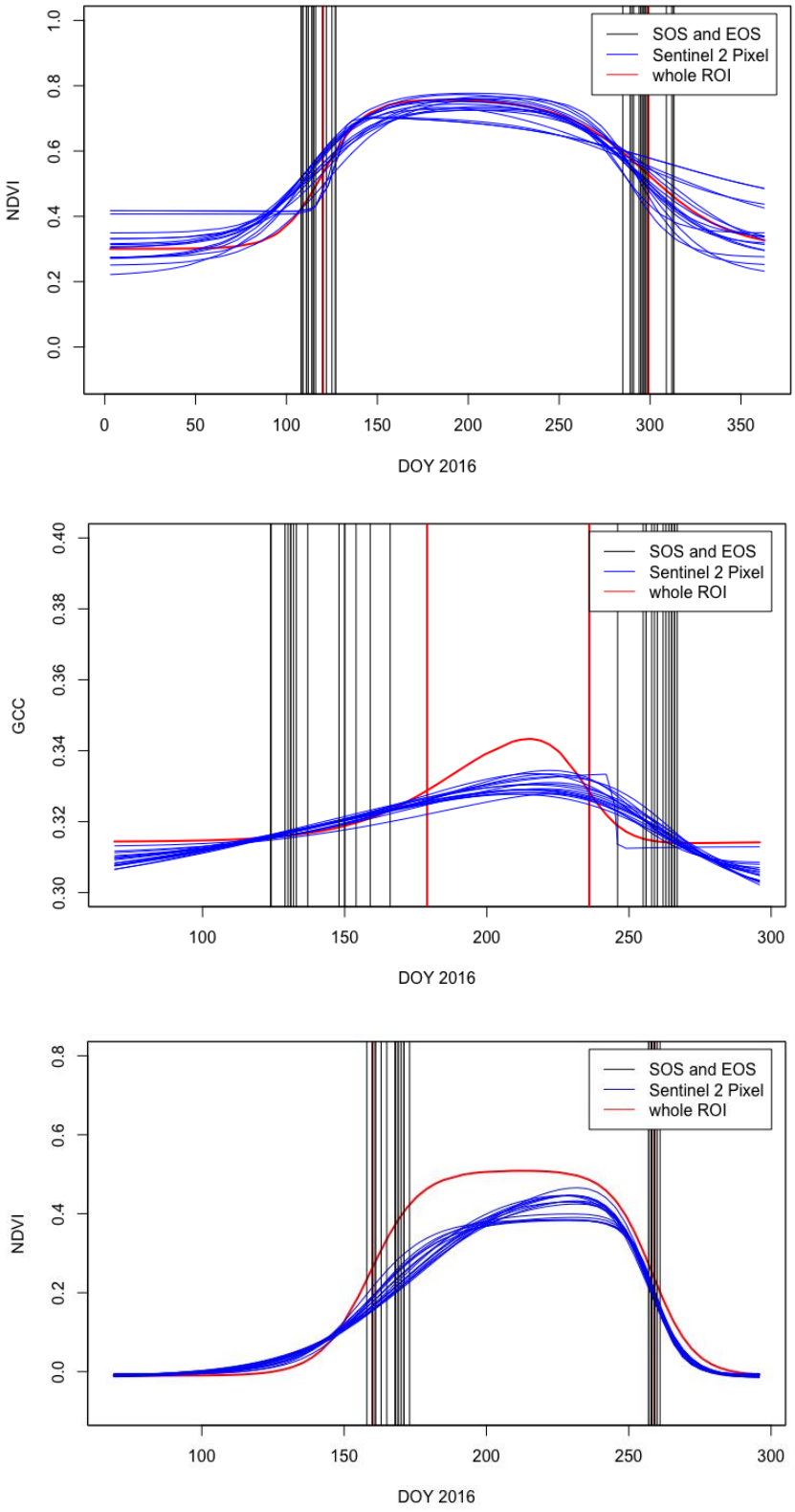

Figure C.4: Pixel-wise analysis of Sentinel-2 GCC and NDVI data at Laegern (top) and Kytalyk test site 2015 (middle) and 2016 (bottom).

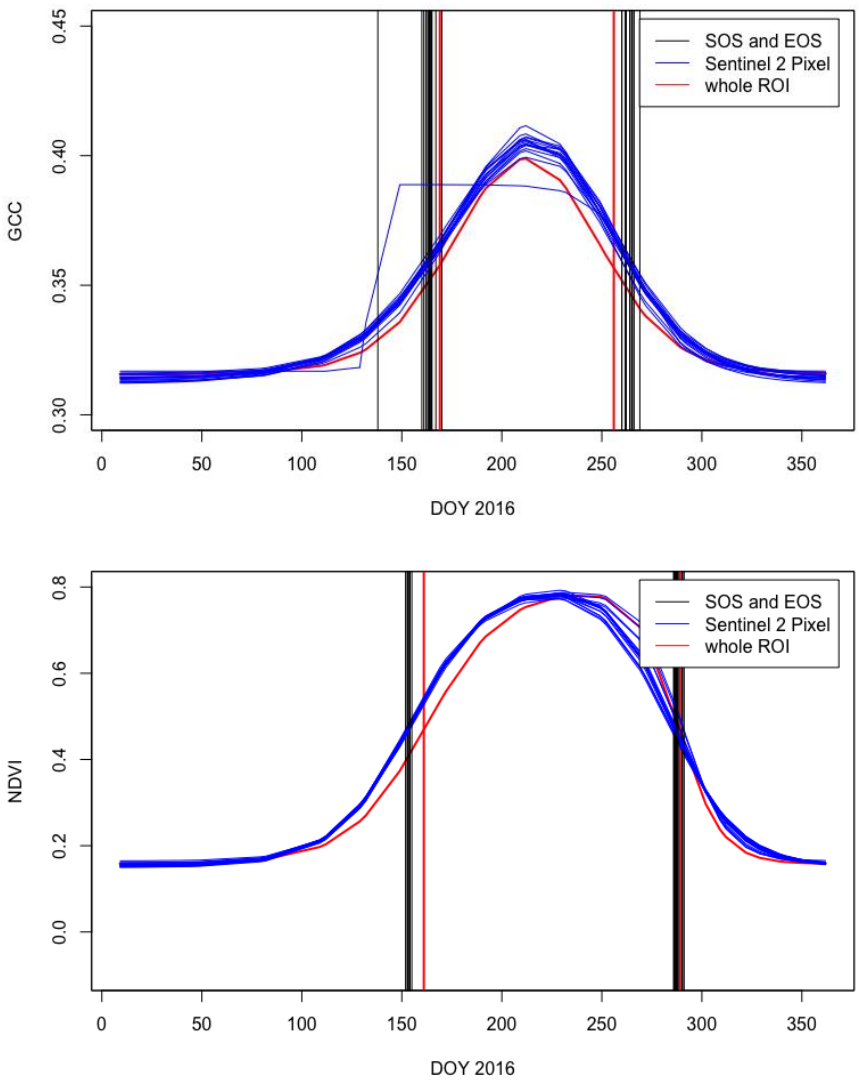

Figure C.5: Pixel-wise analysis of Sentinel-2 GCC and NDVI data at Haibei test site 2015 (top) and 2016 (bottom). Due to an issue with the fitting algorithm an outlier curve occurred (upper graph).

D: NDVI and GCC Comparison

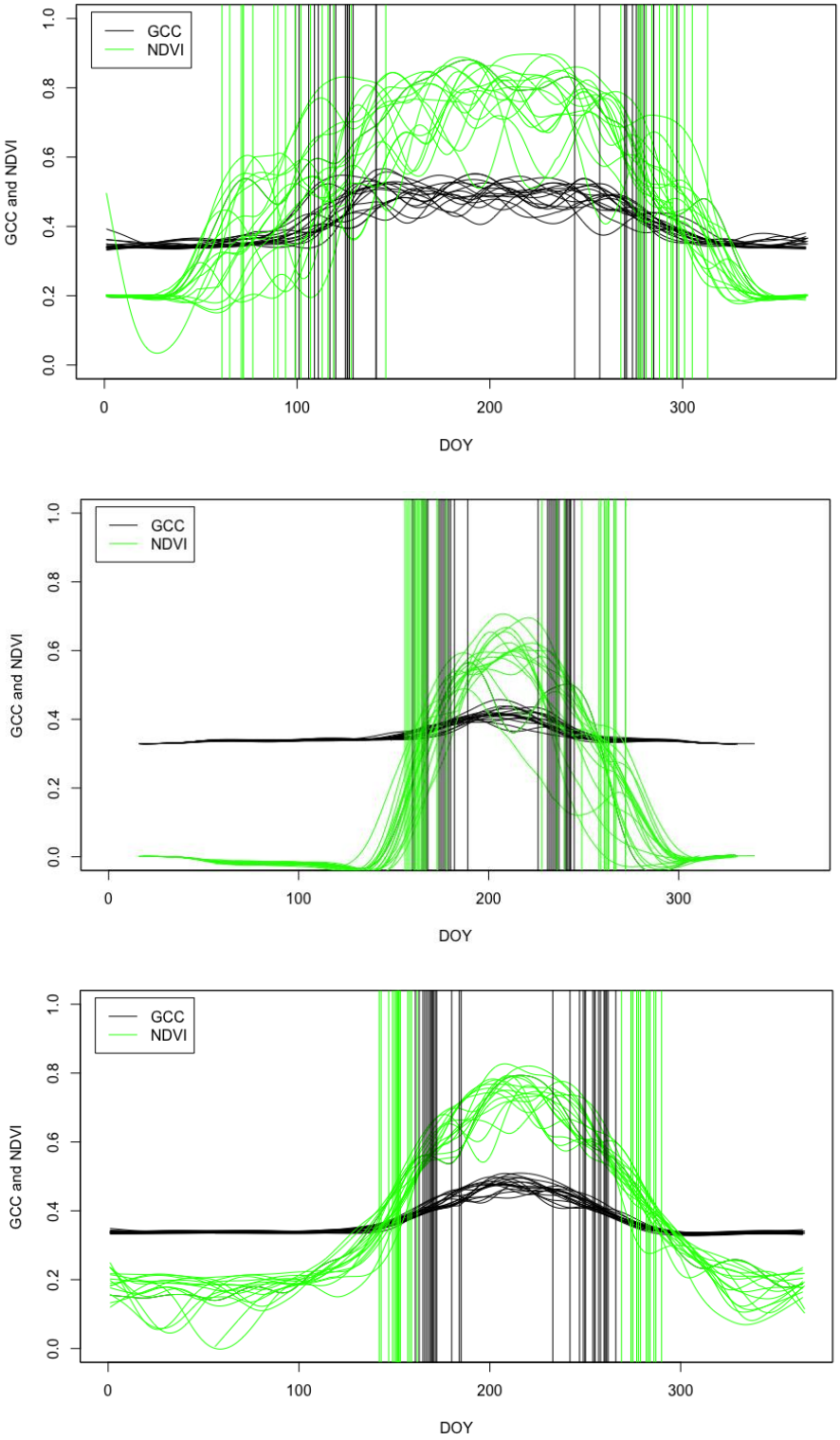

Figure D.6: MODIS GCC (black) and NDVI (green) data from 2000 to 2016 at Laegern (top), Kytalyk (middle) and Haibei (bottom) test site.

Table D-7: Time-series of MODIS GCC and NDVI data for Laegern, Kytalyk and Haibei test site. Metrics are indicated as day of year. Minimal (Min) and maximal (Max) value, the mean of all measurements, the range between min and max and the standard deviation (Stdev) are indicated at the bottom of the table.

	Laegern				Kytalyk				Haibei			
	SOS		EOS		SOS		EOS		SOS		EOS	
Year	**GCC**	**NDVI**	**GCC**	**NDVI**	**GCC**	**NDVI**	**GCC**	**NDVI**	**GCC**	**NDVI**	**GCC**	**NDVI**
2000	141	90	270	295	175	167	241	266	170	90	255	283
2001	127	128	244	305	177	163	231	236	185	162	255	274
2002	126	71	278	284	176	167	242	267	163	152	257	282
2003	111	72	280	295	189	178	233	249	167	157	266	277
2004	127	107	271	279	182	173	243	261	170	152	262	284
2005	126	94	277	277	167	156	237	263	172	147	260	275
2006	125	119	297	313	161	158	226	228	161	143	258	290
2007	99	88	284	292	168	161	243	266	169	149	242	269
2008	117	116	277	298	179	173	243	272	168	142	261	286
2009	106	99	285	294	174	164	232	258	180	158	250	283
2010	141	102	270	301	167	165	245	263	184	159	254	274
2011	99	77	281	288	178	166	236	259	165	153	249	277
2012	120	61	274	278	167	157	234	263	172	152	260	279
2013	129	146	257	268	160	159	236	240	166	153	247	282
2014	101	65	285	295	180	162	235	272	170	151	261	287
2015	109	72	286	281	166	163	241	262	171	152	250	278
2016	119	100	278	355	165	161	240	261	169	151	233	283
Min	99	61	244	268	160	156	226	228	161	90	233	269
Max	141	146	297	355	189	178	245	272	185	162	266	290
Mean	119.00	94.53	276.12	294.00	172.41	164.29	237.53	258.00	170.71	148.41	254.12	280.18
Range	42	85	53	87	29	22	19	44	24	72	33	21
Stdev	13.21	23.75	12.00	19.41	8.02	6.01	5.28	12.50	6.65	15.92	8.28	5.46
R^2	0.1399		-0.0321		0.6584		0.4914		0.4354		-0.0146	

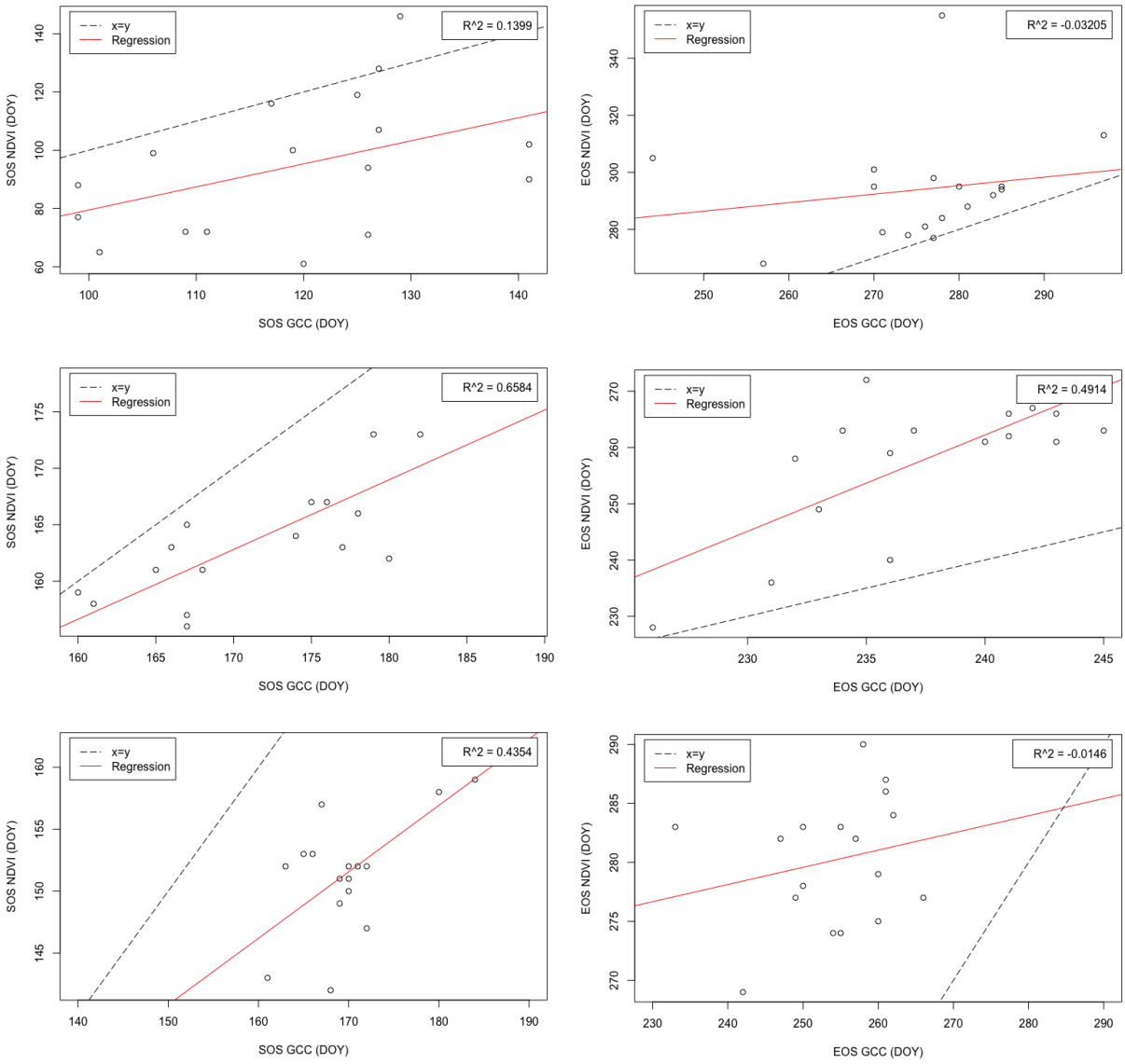

Figure D.7: Linear regressions of the MODIS time series from 2000 to 2016, depicting the correlation between GCC and NDVI metrics at Laegern (top), Kytalyk (middle) and Haibei (bottom) for the SOS (left) and EOS (right).

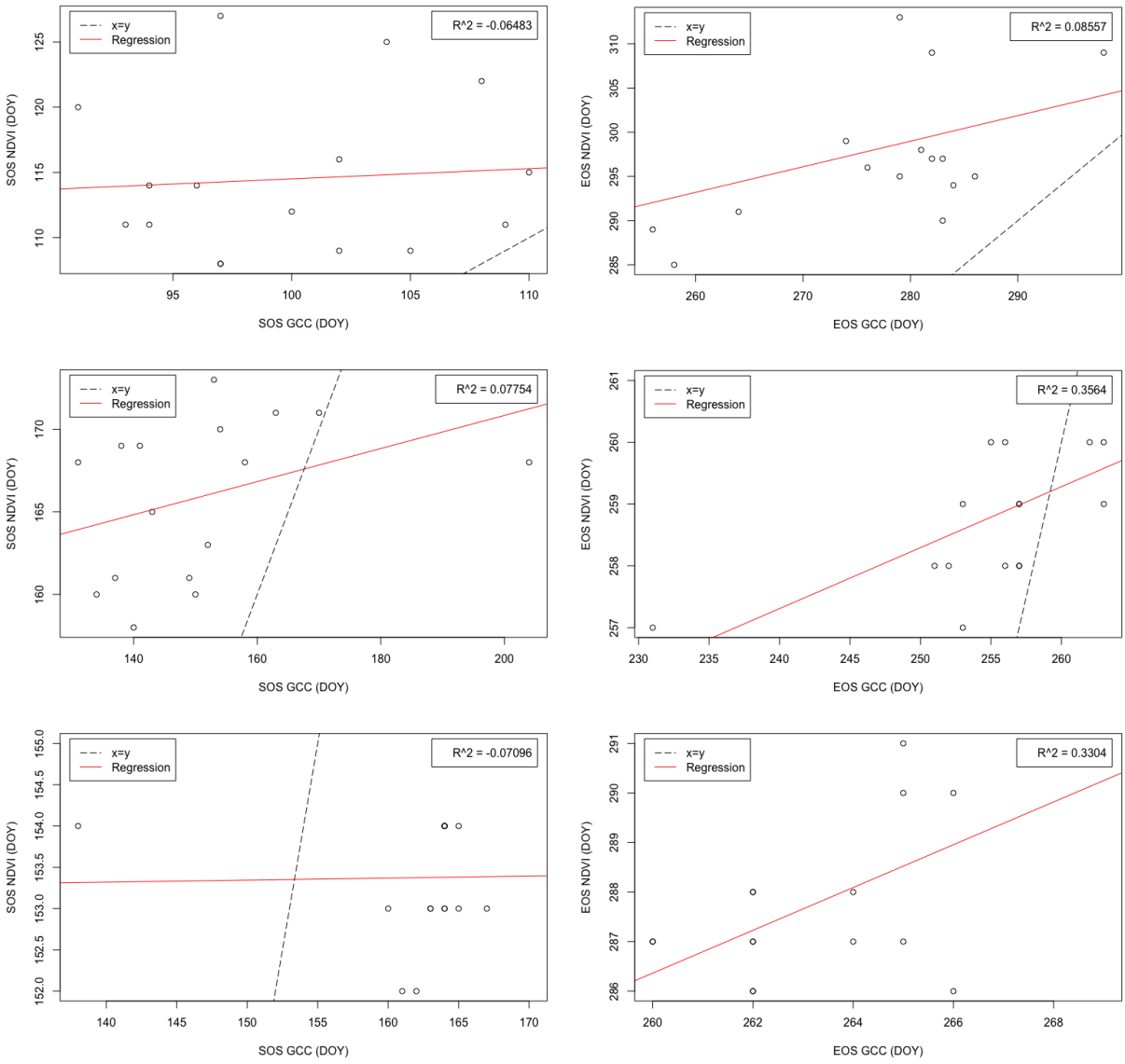

Figure D.8: Linear regressions for the correlation of the GCC and NDVI metrics for the pixel-wise analysis at Laegern (top), Kytalyk (middle) and Haibei (bottom) for the SOS (left) and EOS (right).

E: Code

The files, containing the code to export and extract the data and to process them, are enclosed as external files.

Google Earth Engine (GEE)

-GEE time series:

https://code.earthengine.google.com/e07698d6724e31299b606c56b3b86713

-GEE test sites:

https://code.earthengine.google.com/717a30c099588d90e983522ff750bc2c

Table E-8: Overview of the filenames containing the code used for this thesis (R and PyCharm software) The application of the code is depicted in Figure 3.1.

		Phenocam Images	**Satellite Imagery**
PyCharm			-ExportEEcollection.py
R	Preparation	-Phenopix_installer.R	
	Main files	-testsite_configPC.R -draw_ROI.R	-testsite_configuration.R
	Required functions	-calculate_VIs.R -PhenoMetricsPC.R -calculateSOSEOS.R -plotPhenoRois.R	-ReadTiff.R -mergeDatasets.R -PhenoMetricsSat.R -calculateSOSEOS.R -plots2p.R -plot_data.R -GCCNDVIts.R

Declaration of Originality

Personal declaration: I hereby declare that the submitted thesis is the result of my own, independent work. All external sources are explicitly acknowledged in the thesis.

Date, Place

Signatory